The American Journal of Human Genetics, Volume *90*

Supplementary Data

Age-Related Somatic Structural Changes

in the Nuclear Genome of Human Blood Cells

Lars A. Forsberg, Chiara Rasi, Hamid R. Razzaghian, Geeta Pakalapati, Lindsay Waite, Krista Stanton Thilbeault, Anna Ronowicz, Nathan E. Wineinger, Hemant K. Tiwari, Dorret Boomsma, Maxwell P. Westerman, Jennifer R. Harris, Robert Lyle, Magnus Essand, Fredrik Eriksson, Themistocles L. Assimes, Carlos Iribarren, Eric Strachan, Terrance P. O'Hanlon, Lisa G. Rider, Frederick W. Miller, Vilmantas Giedraitis, Lars Lannfelt, Martin Ingelsson, Arkadiusz Piotrowski, Nancy L. Pedersen, Devin Absher, and Jan P. Dumanski

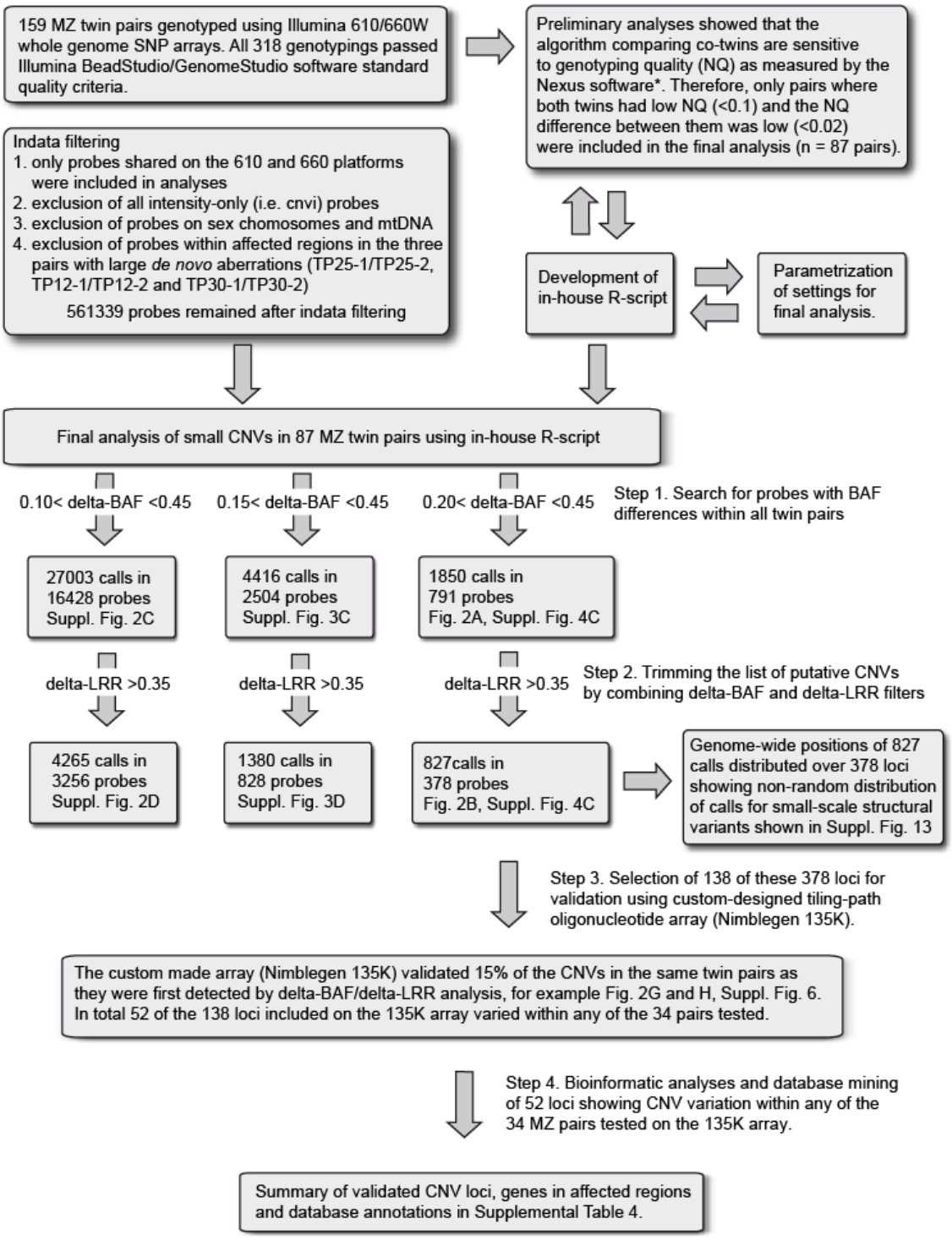

Figure S1. Flowchart Describing Analysis Pipeline for Small-Scale *de novo* Copy Number Variable (CNV) Loci using Cohorts of Age Stratified MZ Twins

By analyzing B-Allele Frequency (BAF) and Log R Ratio (LRR) from the Illumina SNP array analysis of 159 MZ twin pairs, we could identify and validate 52 CNV loci (Table S4). The analysis algorithm was developed in R version 2.12.0. Asterisk (*) indicates Nexus Copy Number 5 Discovery Edition

program (BioDiscovery Inc., CA, USA), which was initially used for analysis of array-data. The Nexus quality score (i.e. NQ) is an estimate of statistical variance of the differences in the intensity data (LRR) of adjacent probes after removing 3% outlying values.

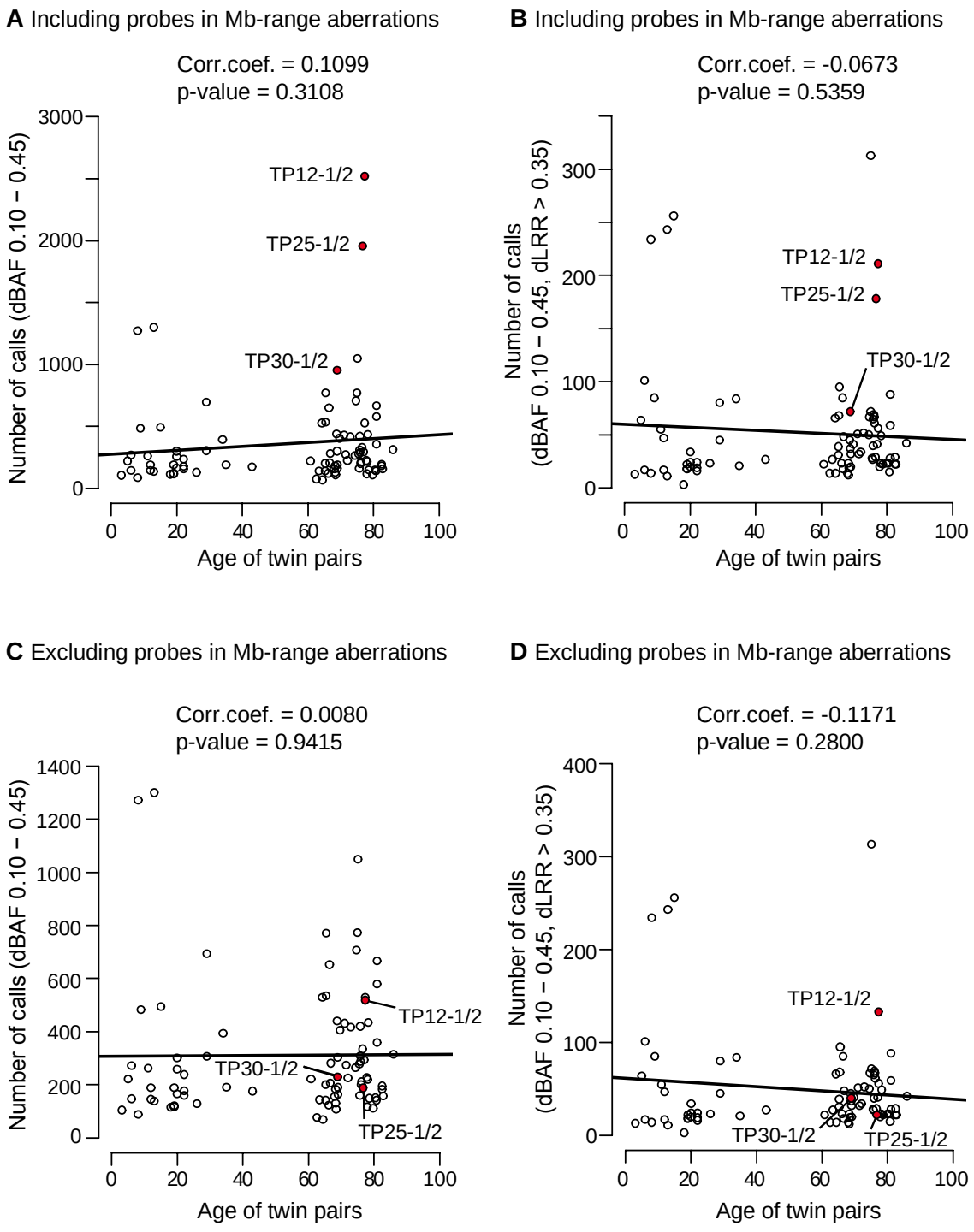

Figure S2. Testing of Filtering Parameters for Detection of Small Somatic Structural Rearrangements in 87 Pairs of MZ Twins using Delta-BAF Filter of 0.10 to 0.45

The settings applied in this version of the filter did not eliminate random noise in the data-set, when compared with the filter settings showed in Figures S3 and S4. Results in panels (A) and (B) are plotted including loci within three known large-scale de novo aberrations (red-dots; pair TP12-1/TP12-2 containing a terminal CNN-LOH, 76.47 Mb on 10q, pair TP25-1/TP25-2 with a 32.46 Mb deletion on 5q, and pair TP30-1/TP30-2 with a 12.91 Mb deletion on 20q) and in panels (C) and (D) the same data are plotted without the probes of these well-characterized and validated large-scale aberrations. These three MZ pairs were suitable internal controls, allowing testing of whether the filters at different settings were discerning the three large-scale aberrations, thus allowing us to test the sensitivity of the method (for more information see Figure S4). Supplemental Figures 3 and 4 have similar set-up with testing filters at different thresholds, with and without inclusion of probes located within the large aberrations. Panels (A) and (C) are showing data after filtering of intra-pair differences using delta-BAF filter only and panels (B) and (D) show results using delta-BAF in combination with delta-LRR filters. Each dot represents data from one MZ twin pair.

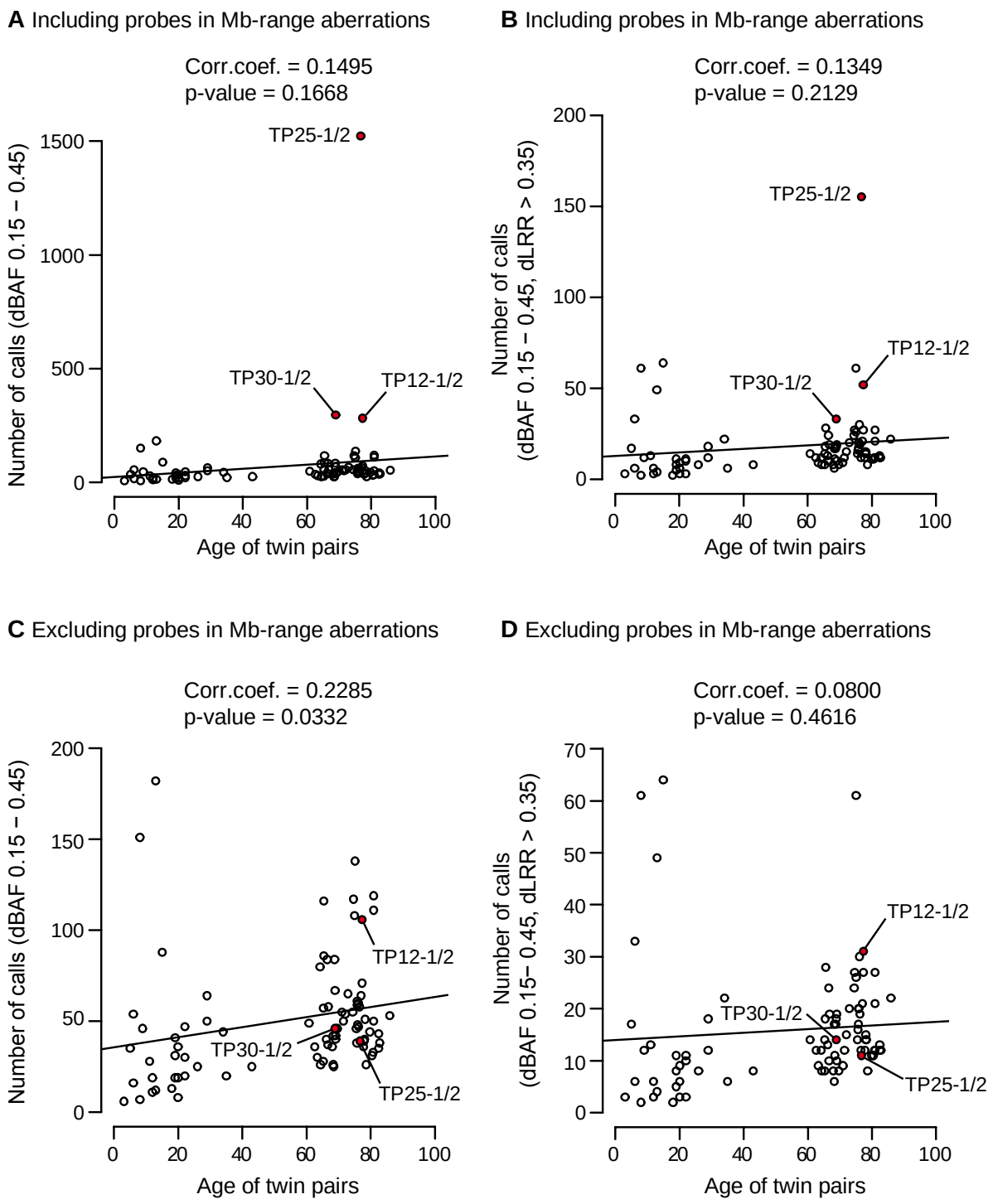

Figure S3. Testing of Filtering Parameters for Detection of Small Somatic Structural Rearrangements in 87 Pairs of MZ Twins using Delta-BAF Filter of 0.15 to 0.45

These settings filtered out random noise in a more efficient way as compared to 0.10 to 0.45 settings in Figure S2, but not to the same extent as 0.20 to 0.45 settings shown in Figure S4. This figure has a similar set up as Figures S2 and S4. Results in (A) and (B) are plotted including loci within three known large-scale de novo aberrations (red-dots; pair TP12-1/TP12-2 containing a terminal CNN-LOH of 76.47 Mb on 10q, pair TP25-1/TP25-2 with a 32.46 Mb deletion on 5q, and pair TP30-1/TP30-

2 with a 12.91 Mb deletion on 20q) and in panels (C) and (D) the same data are plotted without the probes for these known aberrations (for more information see Figure S4). Panels (A) and (C) are showing data after filtering of intra-pair differences using delta-BAF filter only and panels (B) and (D) show results using delta-BAF in combination with delta-LRR filters. Each dot represents data from one MZ twin pair.

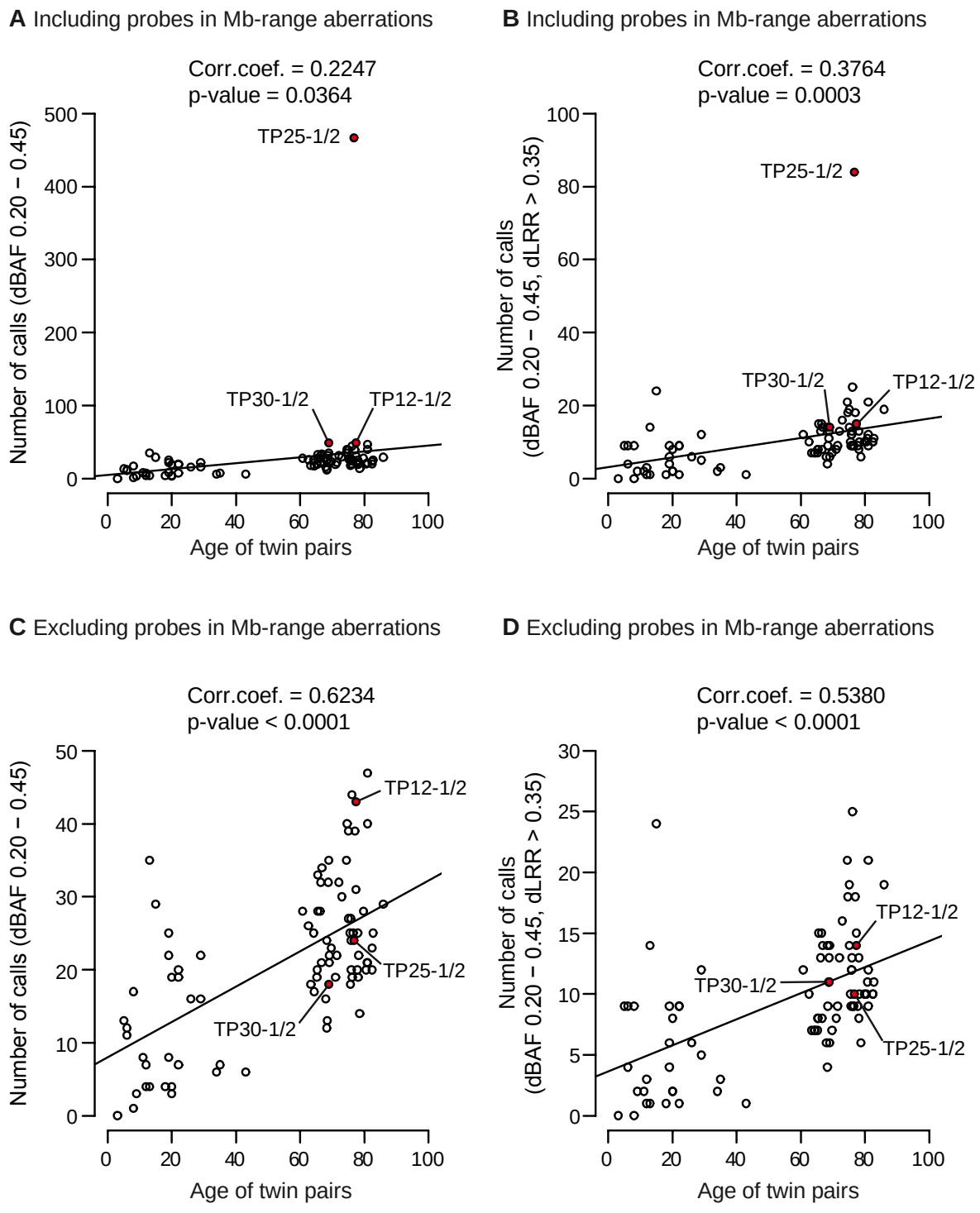

Figure S4. Testing of Filtering Parameters for the Detection of Small Somatic Structural Rearrangements in 87 Pairs of MZ Twins using Delta-BAF Filter of 0.20 to 0.45

These settings filtered out random noise in the most optimal way, when compared to settings in Figures S2 and S3. Each dot represents data from one MZ twin pair and panels (A) and (C) show intra-pair differences using the delta-BAF filter only, while panels (B) and (D) show data using delta-BAF in combination with delta-LRR filters. Results in (A) and (B) are plotted including loci within three known large-scale de novo aberrations (red-dots; pair TP12-1/TP12-2 containing a terminal CNN-LOH of 76.47 Mb on 10q, pair TP25-1/TP25-2 with a 32.46 Mb deletion on 5q, and pair TP30-1/TP30-2 with a 12.91 Mb deletion on 20q) and in panels (C) and (D) the same data are plotted without the probes in these known aberrations. These three MZ pairs are suitable internal controls, allowing testing of whether the filters at different settings were discerning the three large-scale aberrations, thus allowing us to test the sensitivity of the pipeline shown in Figure S1. The filter setting “delta-BAF 0.20 to 0.45” with inclusion of probes in the three large scale aberrations is identifying CNVs in all three cases (A). Twin TP25-2 has the highest proportion of cells (50.5%) with CNV and the deletion is very large (32.46 Mb) in size. This pair is therefore showing significantly larger number of calls, when compared with the other twin pair containing deletion (TP30-1/TP30-2, 12.91 Mb). This latter twin pair is, however, at the top of the cloud of calls in panel (A). The level of deletion in twin TP30-1 is estimated to 41.5% of cells affected with one copy loss. In summary, these results are in agreement with the qPCR validation for deletions in twin TP30-1 and twin TP25-2 (Figure 5). Data shown here in panels (C) and (D) are also shown in Figure 2, panels (A) and (B), respectively.

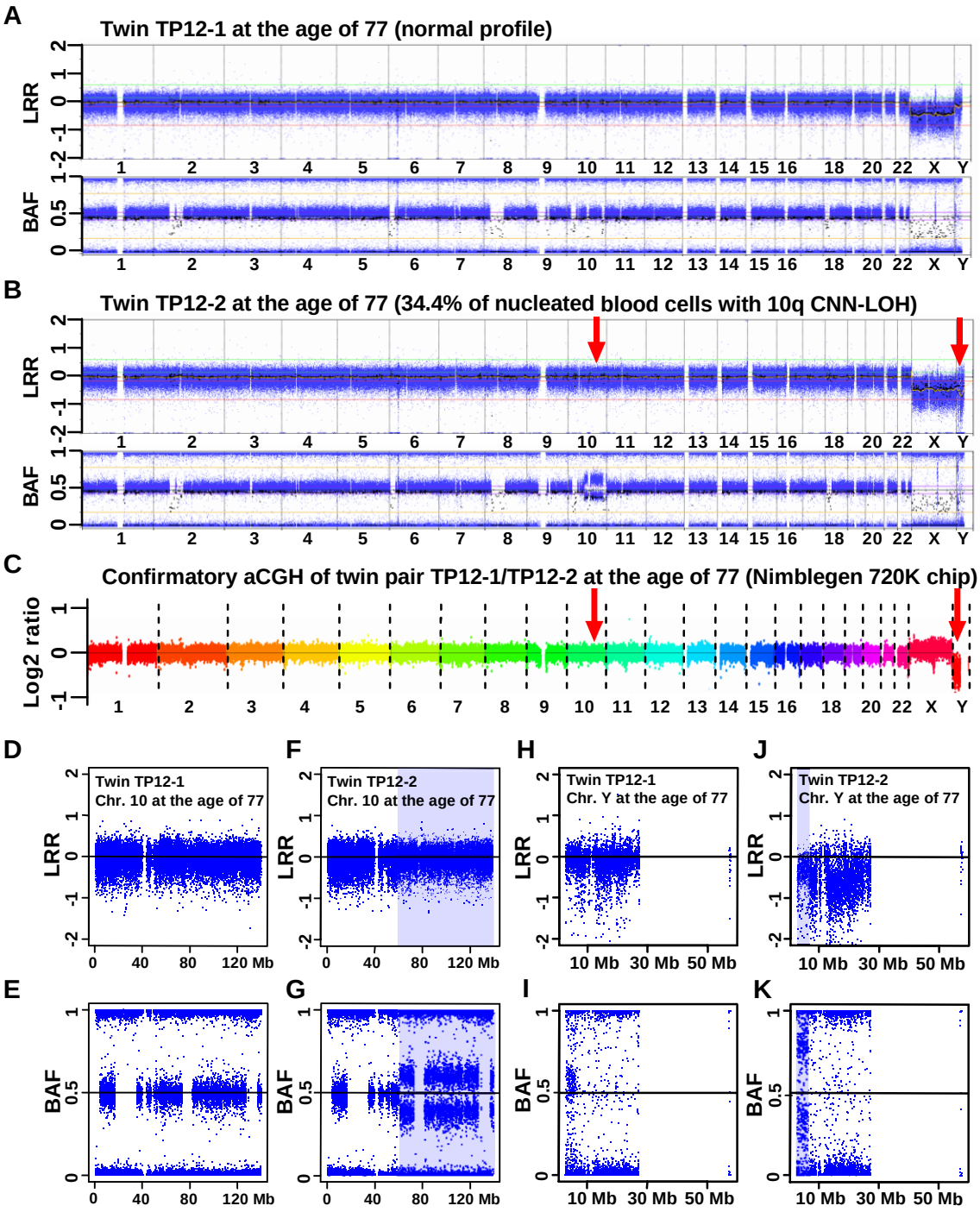

Figure S5. Two Large-Scale Genetic Aberrations Found in a 77-Year-Old MZ Twin TP12-2 using the Illumina SNP Array

Twin TP12-1 shows a normal copy number profile (A, D, and E). Using B-Allele Frequency (BAF) a 76.5 Mb large copy number neutral loss of heterozygosity (CNN-LOH) was identified on 10q in co-twin TP12-2 (B, F, and G). Quantification of cells containing the CNN-LOH using the MAD package suggests that 34.4% of cells were affected. As expected, comparative genomic hybridization array (aCGH) could not detect this copy number neutral aberration (C). However, the TP12-2 twin also showed a monosomy of chromosome Y in a proportion of cells (B, J, and K) and this CNV was

confirmed using aCGH (C). Three Illumina platforms (600K, 1M-Duo and 1M Omni) were used in the primary detection and validation of the results from this twin pair (details not shown).

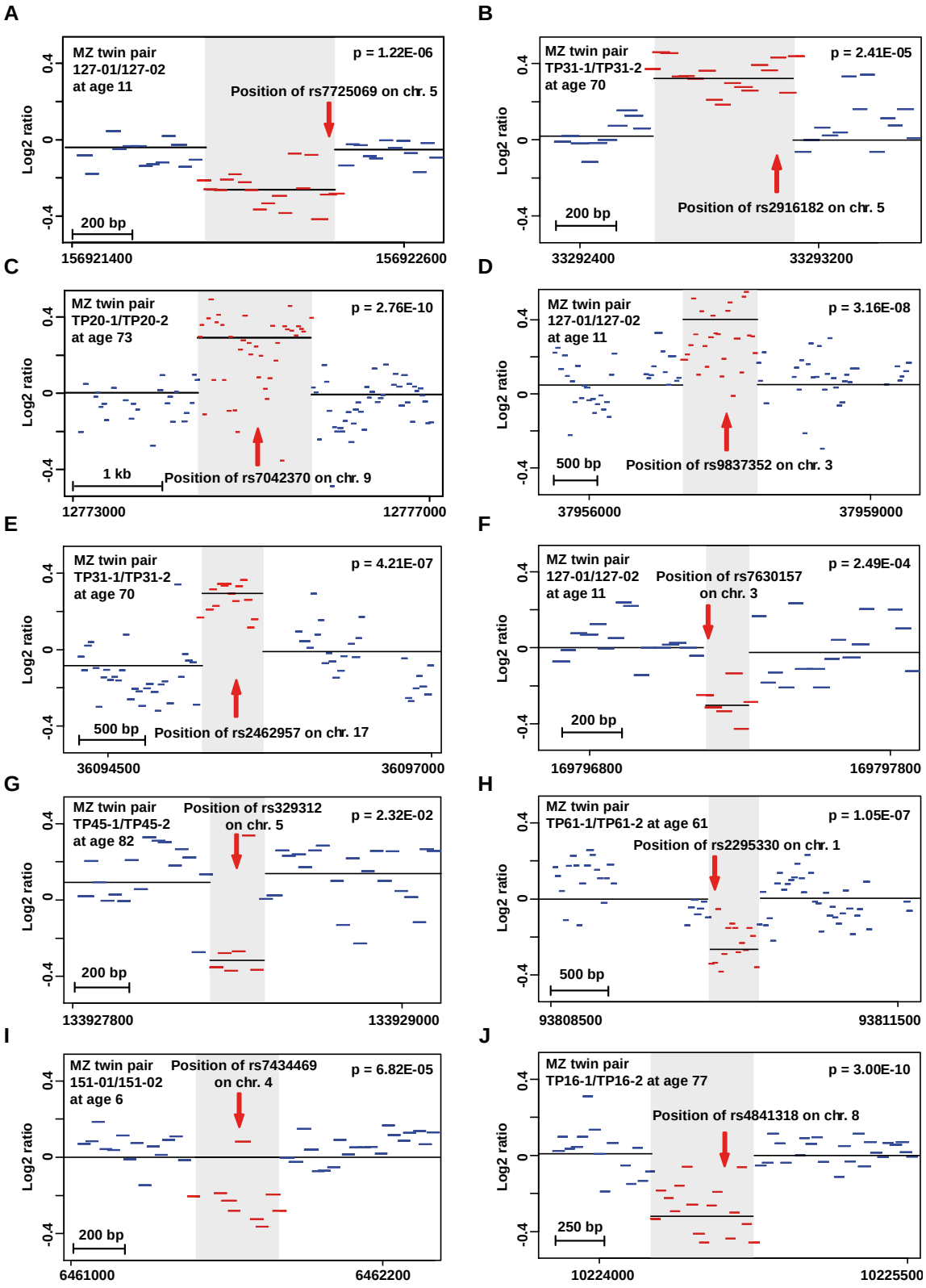

Figure S6 (1/2)

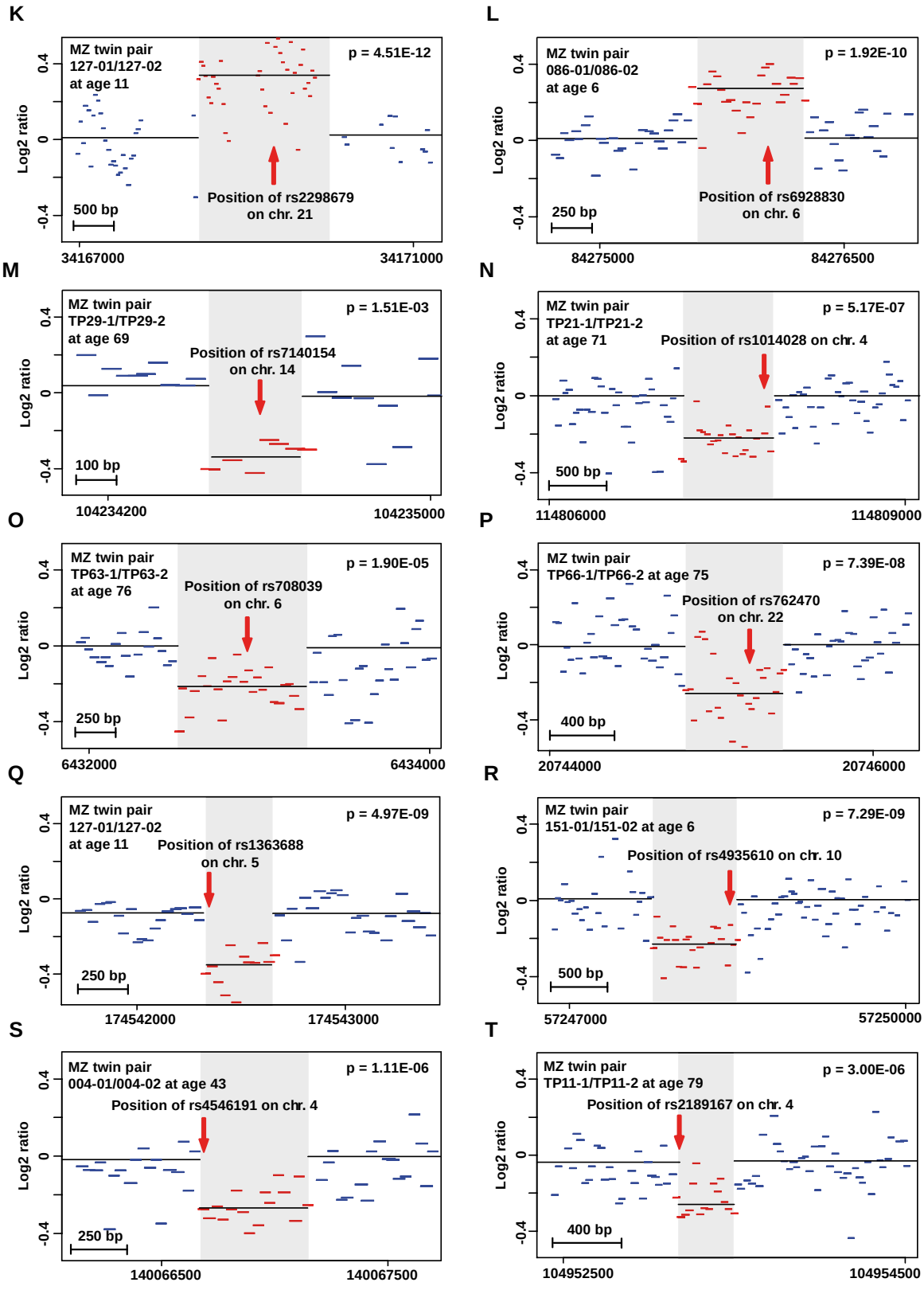
K
MZ twin pair
127-01/127-02
at age 11
p = 4.51E-12
Position of rs2298679
on chr. 21
500 bp
34167000
34171000
L
MZ twin pair
086-01/086-02
at age 6
p = 1.92E-10
Position of rs6928830
on chr. 6
250 bp
84275000
84276500
M
MZ twin pair
TP29-1/TP29-2
at age 69
p = 1.51E-03
Position of rs7140154
on chr. 14
100 bp
104234200
104235000
N
MZ twin pair
TP21-1/TP21-2
at age 71
p = 5.17E-07
Position of rs1014028 on chr. 4
500 bp
114806000
114809000
O
MZ twin pair
TP63-1/TP63-2
at age 76
p = 1.90E-05
Position of rs708039
on chr. 6
250 bp
6432000
6434000
P
MZ twin pair
TP66-1/TP66-2 at age 75
p = 7.39E-08
Position of rs762470
on chr. 22
400 bp
20744000
20746000
Q
MZ twin pair
127-01/127-02
at age 11
p = 4.97E-09
Position of rs1363688
on chr. 5
250 bp
174542000
174543000
R
MZ twin pair
151-01/151-02 at age 6
p = 7.29E-09
Position of rs4935610 on chr. 10
500 bp
57247000
57250000
S
MZ twin pair
004-01/004-02 at age 43
p = 1.11E-06
Position of rs4546191 on chr. 4
250 bp
140066500
140067500
T
MZ twin pair
TP11-1/TP11-2 at age 79
p = 3.00E-06
Position of rs2189167 on chr. 4
400 bp
104952500
104954500
Log2 ratio
0.4
0
-0.4

Figure S6 (2/2)

Figure S6.

Validation of small-scale putative CNVs by array-comparative genomic hybridization using custom-made maximum-resolution tiling-path oligonucleotide array (Nimblegen 135K) using co-twins (A–T). Statistical significance for the results from the Nimblegen array was calculated using the Mann-Whitney U-test, analyzing values for region of interest (shaded) and on both sides flanking control regions. By co-hybridization of monozygotic twins we could successfully validate 52 (38%) loci displaying putative small-scale CNVs. The custom-made 135K Nimblegen array consisted of 137545 probes, which were used to validate the 138 putative CNV loci detected by the Illumina SNP array (Figure 2B and Figures S1 and S4D). In total, the design consisted of 98894 experimental probes (covering the chromosomal windows shown in Table S4) and an additional 38651 backbone control probes evenly distributed across the whole genome. Probe sequence length varied according to Nimblegen recommendations between 50 and 75 bps and the median overlap of probes (i.e. probe spacing) was 30 bps. The rate of validation success was not different in the young (n=8) and old (n=26) MZ pairs used in these experiments (t-test, t=0.7062, p-value=0.4819), supporting the results from linear regression analyses in Figure 2B and Figure S4D.

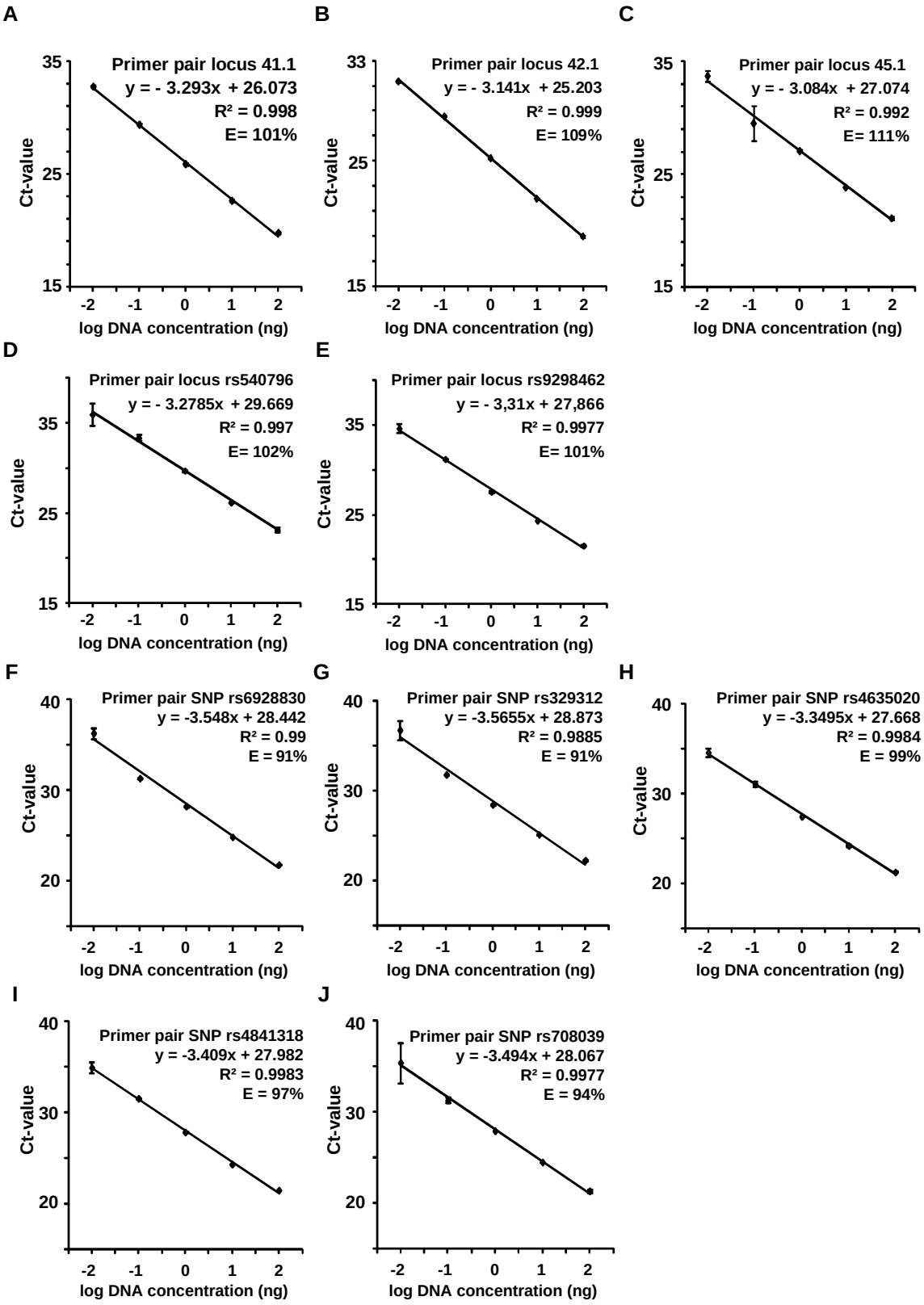
A
Primer pair locus 41.1
y = - 3.293x + 26.073
R² = 0.998
E= 101%
B
Primer pair locus 42.1
y = - 3.141x + 25.203
R² = 0.999
E= 109%
C
Primer pair locus 45.1
y = - 3.084x + 27.074
R² = 0.992
E= 111%
D
Primer pair locus rs540796
y = - 3.2785x + 29.669
R² = 0.997
E= 102%
E
Primer pair locus rs9298462
y = - 3,31x + 27,866
R² = 0.9977
E= 101%
F
Primer pair SNP rs6928830
y = -3.548x + 28.442
R² = 0.99
E = 91%
G
Primer pair SNP rs329312
y = -3.5655x + 28.873
R² = 0.9885
E = 91%
H
Primer pair SNP rs4635020
y = -3.3495x + 27.668
R² = 0.9984
E = 99%
I
Primer pair SNP rs4841318
y = -3.409x + 27.982
R² = 0.9983
E = 97%
J
Primer pair SNP rs708039
y = -3.494x + 28.067
R² = 0.9977
E = 94%
Ct-value
log DNA concentration (ng)

Figure S7. Primer Efficiency of the Primer Pairs Used in the qPCR Experiments

The standard curve of each primer pair and their efficiencies are given in panels A–J. For each primer pair a standard curve was generated by first performing PCR reactions with five known concentrations of control DNA (normal human female genomic DNA; Promega Corporation, Madison, WI, USA). The standard curves were generated by plotting the Ct (Cycle threshold) values from these reactions versus the log DNA concentration of the control DNA. PCR reactions for each DNA concentration were replicated and each point represents the average of Ct values from these reactions. Error bars represents standard deviations from the mean and the PCR efficiency was calculated as: $E=10^{(-1/slope)}-1$.

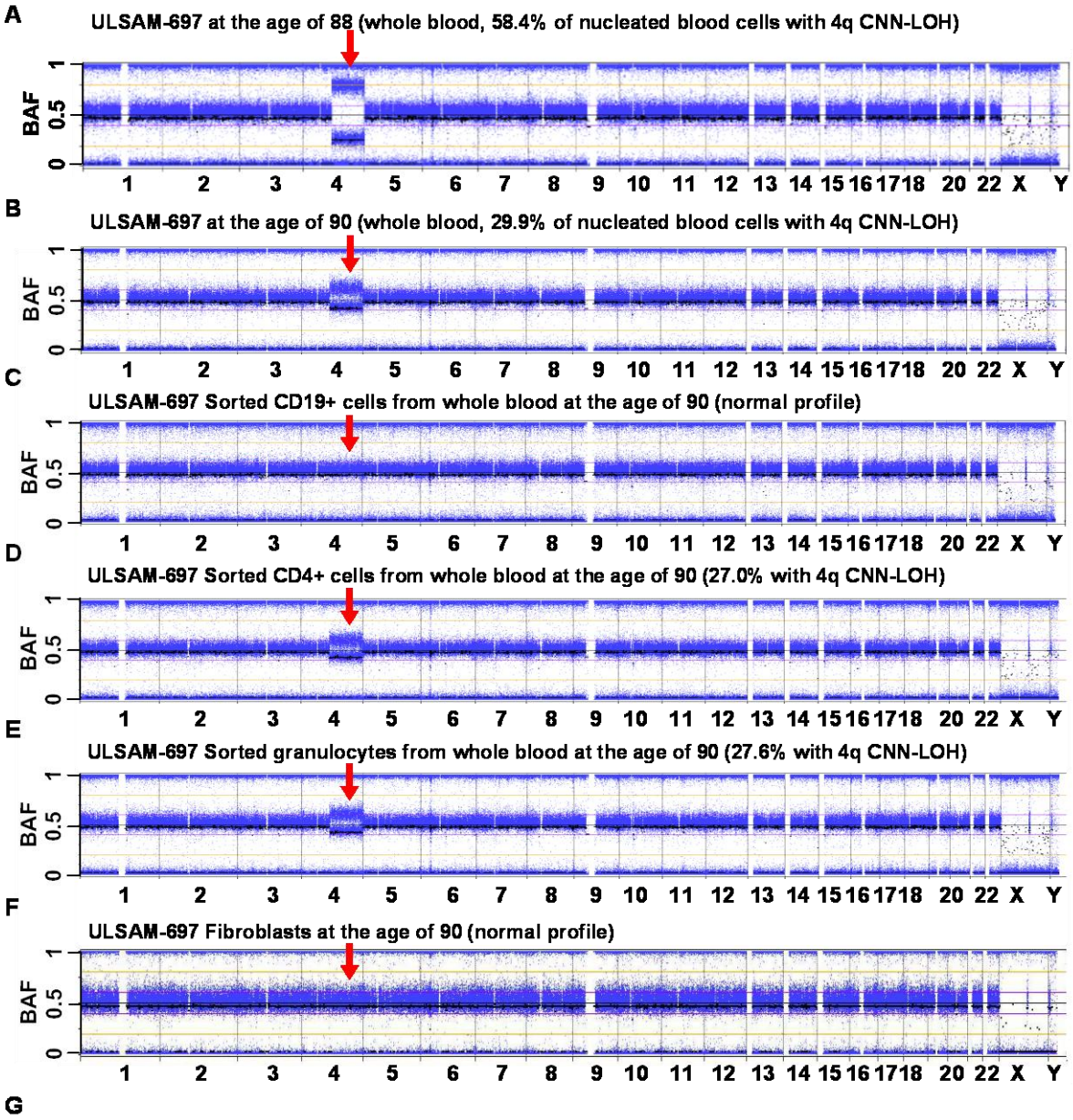

G

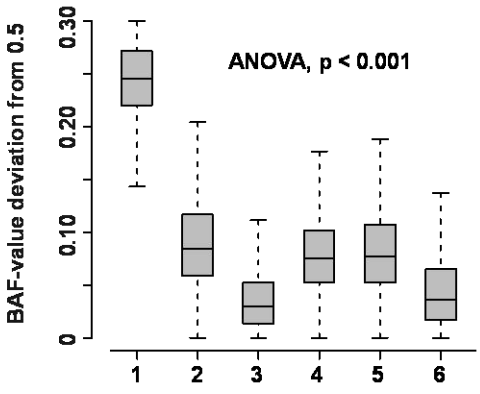

Proportion of cells with 4q CNN-LOH in ULSAM-697

1. Whole blood at the age of 88 = 57.8%
2. Whole blood at the age of 90 = 29.9%
3. CD19+ cells from blood at the age of 90 = 0%
4. CD4+ cells from blood at the age of 90 = 27.0%
5. Granulocytes from blood at the age of 90 = 27.6%
6. Fibroblasts at the age of 90 = 0%

Figure S8. Somatic Event in Sorted Subsets of Blood Cells in the Single-Born ULSAM-697 Subject
A large terminal copy number neutral loss of heterozygozity (CNN-LOH) encompassing 103 Mb of 4q of somatic origin was first detected in the blood sample drawn at 88 years of age, using B-Allele Frequency (BAF) from Illumina SNP array genotyping Panel (A) (see also Figures 1G–1K). Analysis of Illumina data using R-package MAD suggest 58.4% aberrant cells at the age of 88. The subject was re-sampled at the age of 90, when both peripheral blood and a skin biopsy was obtained. The latter was used for short-term culture of fibroblasts. From peripheral blood we sorted CD4+-, CD19+- cells and granulocytes using standard protocols. When comparing whole blood at 88 and 90 years of age, the proportion of cells with CNN-LOH had decreased substantially in only two years (A, B, and G), from 57.8 to 29.9% according to the MAD-estimates. As expected, the fibroblasts sampled as control shows a normal BAF profile without the aberration (F and G). Results from different types of sorted blood cells at the age of 90 showed unexpected results (C–G) and we found significant differences in BAF-deviation between the cell types tested at this age (G, ANOVA; $p<0.001$, Tukey's test for multiple comparisons). Thus, the 4q CNN-LOH was readily detected in CD4+ cells and granulocytes as well as in whole blood, whereas it was absent in CD19+ cells. All estimates of percentages of cells with CNN-LOH presented in this figure were calculated using the MAD package. Analysis of samples taken at the age of 90 was performed in duplicate genotyping experiments on Illumina 1M-Duo and Omni-Express arrays with very similar results.

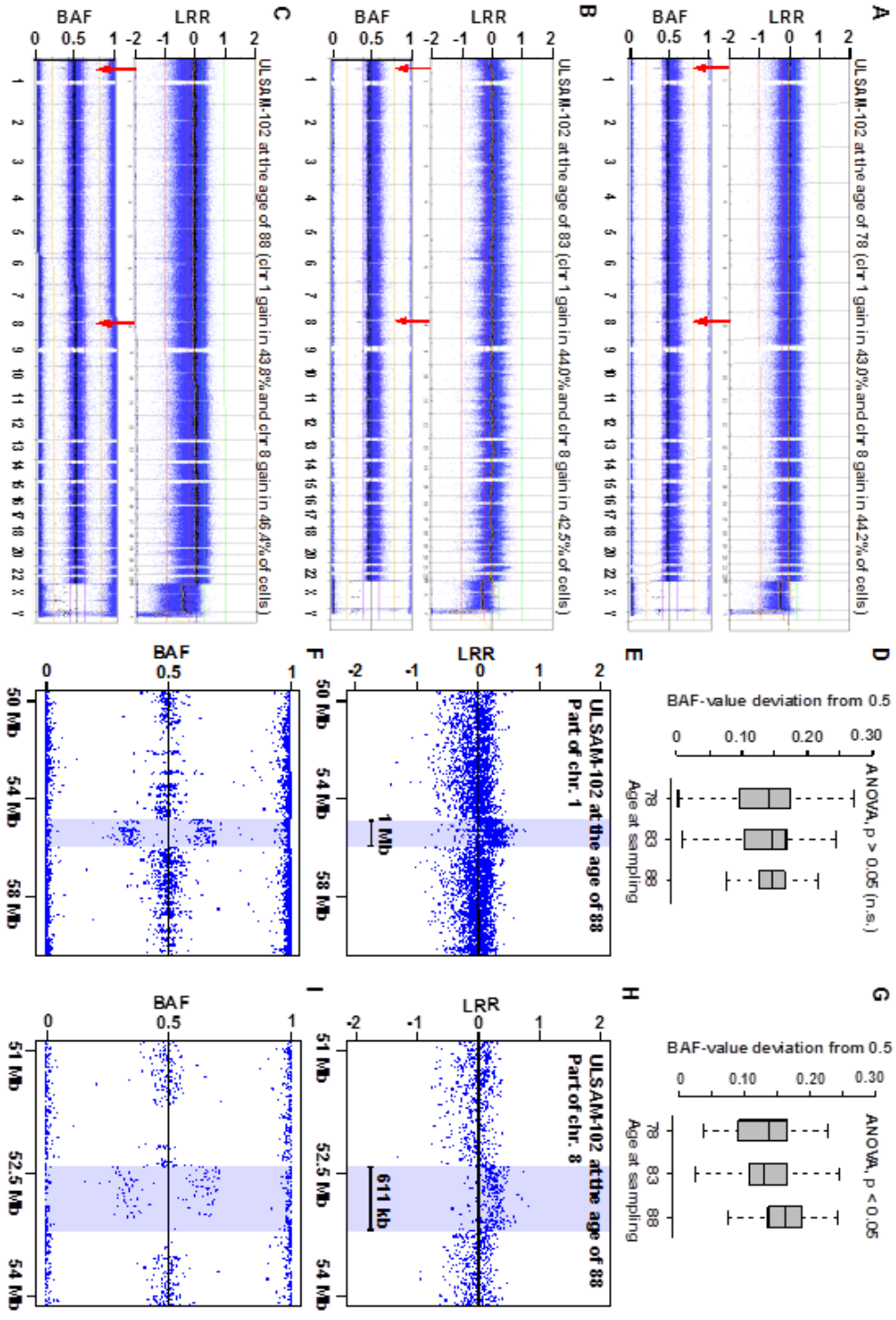

Figure S9. Slow Longitudinal Development of Two Cell Clones Showing Gains in the Single-Born ULSAM-102 Subject, as Detected by Log R Ratio (LRR) and B-Allele Frequency (BAF) using Illumina SNP Array

A 1.09 Mb gain on chromosome 1p shows a relatively stable frequency over a 10 year period of time (A–F, ANOVA, $p>0.05$). Quantification using the MAD package shows that this cell clone contains an aberrant chromosome 1 in ~44 % of cells. The frequency of a cell clone with another aberration (611.3 kb gain on 8q) on the other hand, is slowly increasing over time (A–C, G–I, ANOVA, $p<0.05$).

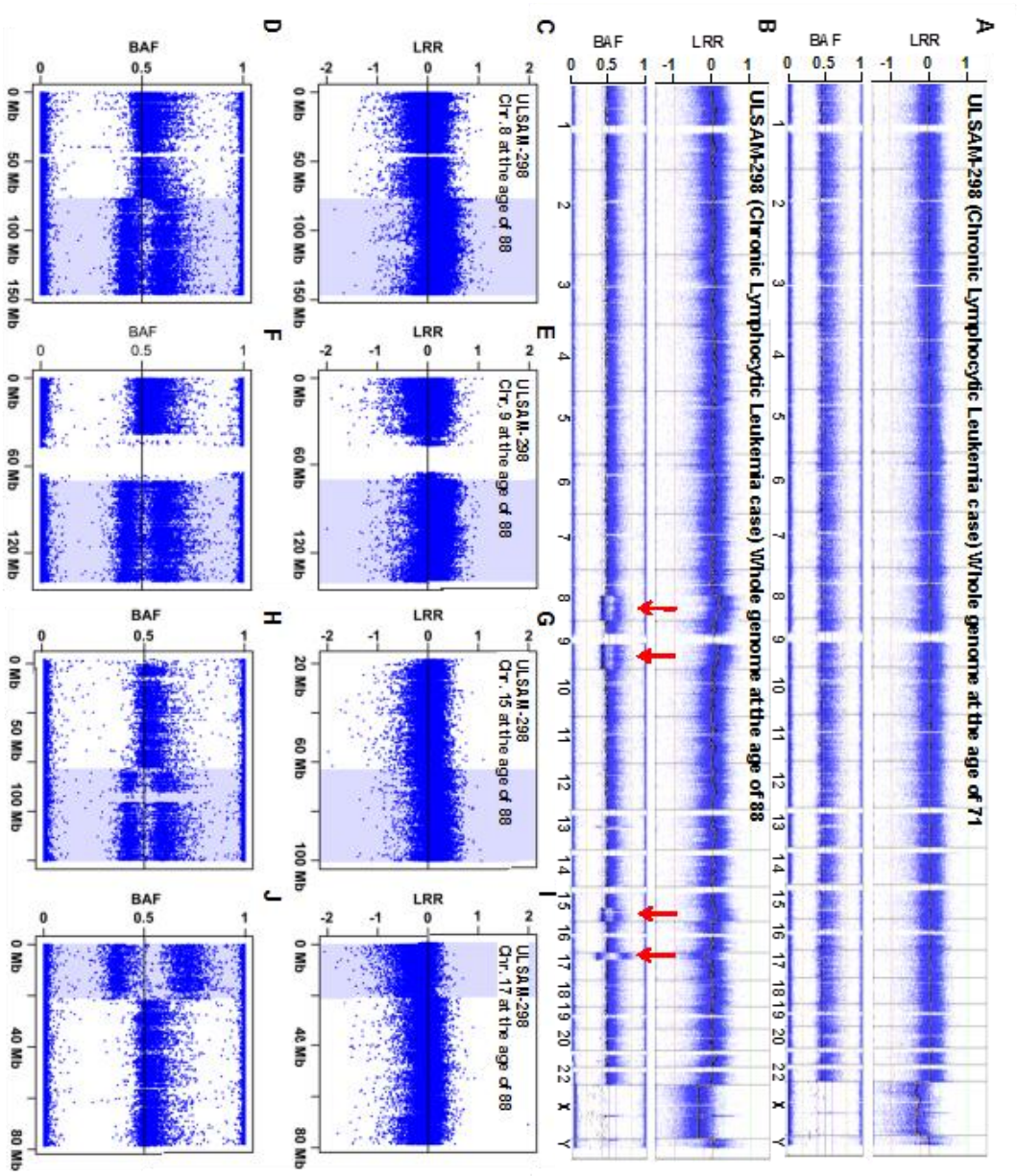

Figure S10. Large Copy Number Aberrations on Multiple Chromosomes Found in Blood from the 88-Year-Old Single-Born ULSAM-298 Subject (B) as Identified by Log R Ratio (LRR) and B-Allele Frequency (BAF) after Illumina SNP Array Analysis

The subject was diagnosed with chronic lymphocytic leukemia (CLL) with anemia and thrombocytopenia at the age of 87 and later prostate cancer with local spread to lymph nodes at the age of 90. No indications of genetic aberrations could be found in the blood drawn at the age of 71 (A).

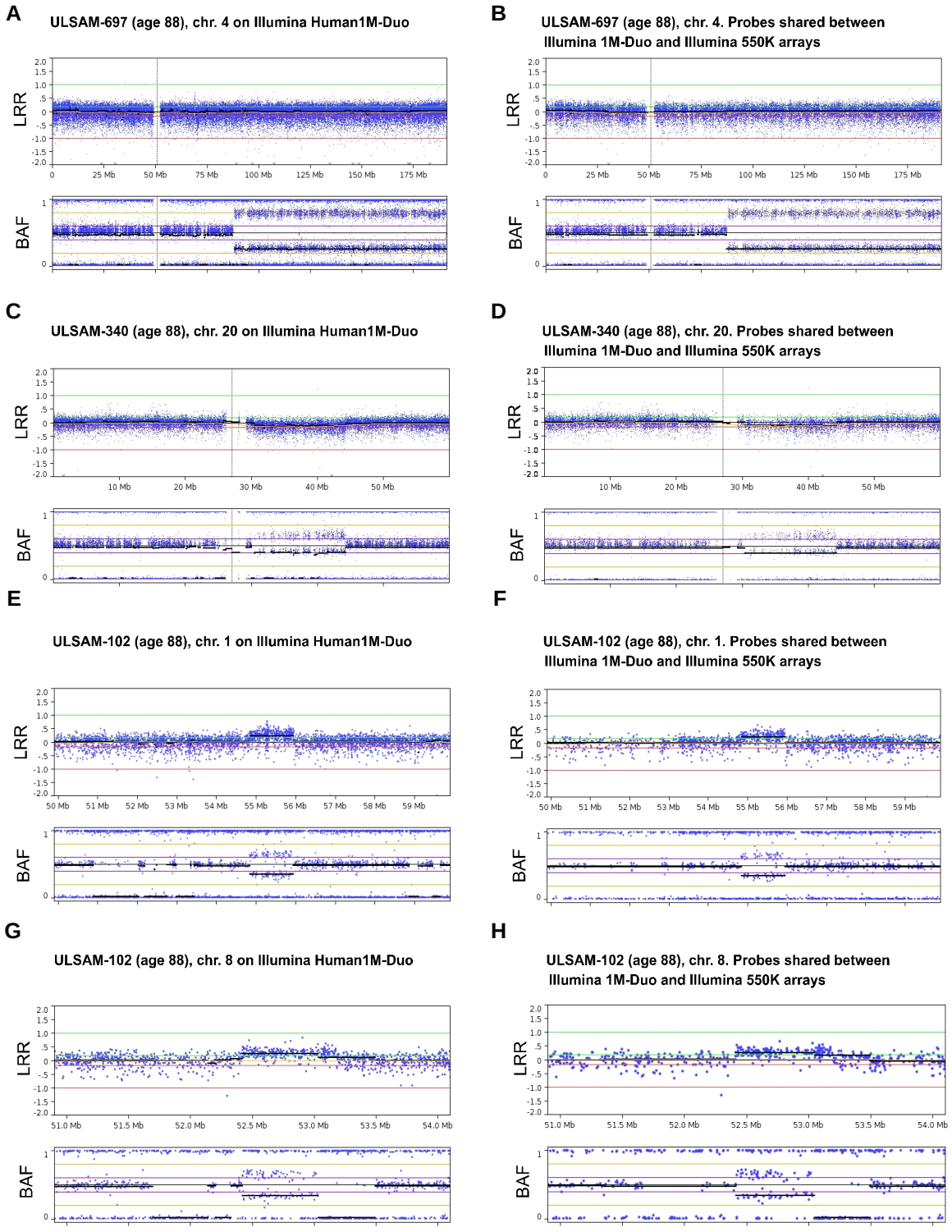

Figure S11. Comparison of Detection Sensitivity for Large-Scale Aberrations Between Illumina 550K Array and Illumina 1M-Duo Array, using Three Subjects From the ULSAM Cohort (ULSAM-697, -340, and -102)

Four structural aberrations uncovered in these three subjects ranged from 611 kb - 103 Mb and encompassed gains, deletion and CNN-LOH. The 550K platform contains 561495 probes of which 99% (557280) are also present on the 1M platform. On the left hand side (panels A, C, E, and G) we

plotted the relevant regions using all probes present in the 1M array. On the right hand side (panels B, D, F, and H) the same regions are plotted only using probes that are shared by both the 1M and the 550K platforms. Even the smallest of these aberrations (661 kb gain on 8q in ULSAM-102) is clearly detectable with probes derived exclusively from 550K array.

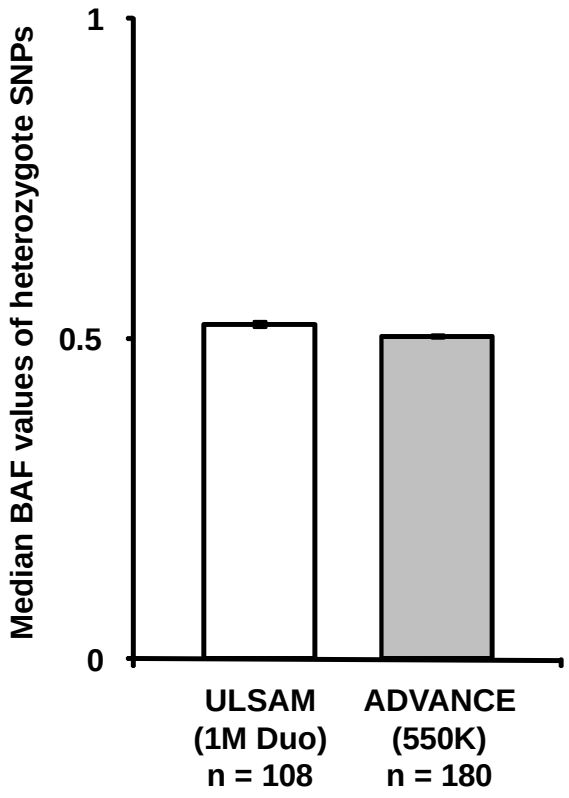

Figure S12. Evaluation of the Overall Genotyping Quality of Illumina 1M-Duo and Illumina 550K Experiments Used in the Analyses of the ULSAM and ADVANCE Cohorts

Plotting of the median BAF-values of heterozygous SNPs for each dataset reliably evaluates the variation in the BAF-values generated by the two platforms. In the ULSAM cohort genotyped on the 1M Duo platform, the median BAF-values of the heterozygote probes were 0.5248 (S.E. ± 0.0042) and the corresponding numbers for the ADVANCE cohort genotyped on the 550K platform were 0.5043 (S.E. ± 0.0023). This analysis shows that the BAF-variation of the 550K genotyping was more close to the theoretically expected 0.5 value, as compared to the 1M Duo results (t-test, $p < 0.001$). Thus, the genotyping quality of ADVANCE cohort is at least as reliable as the results from ULSAM subjects. Error bars indicate standard errors. The raw data summarized in this figure are shown in Table S6.

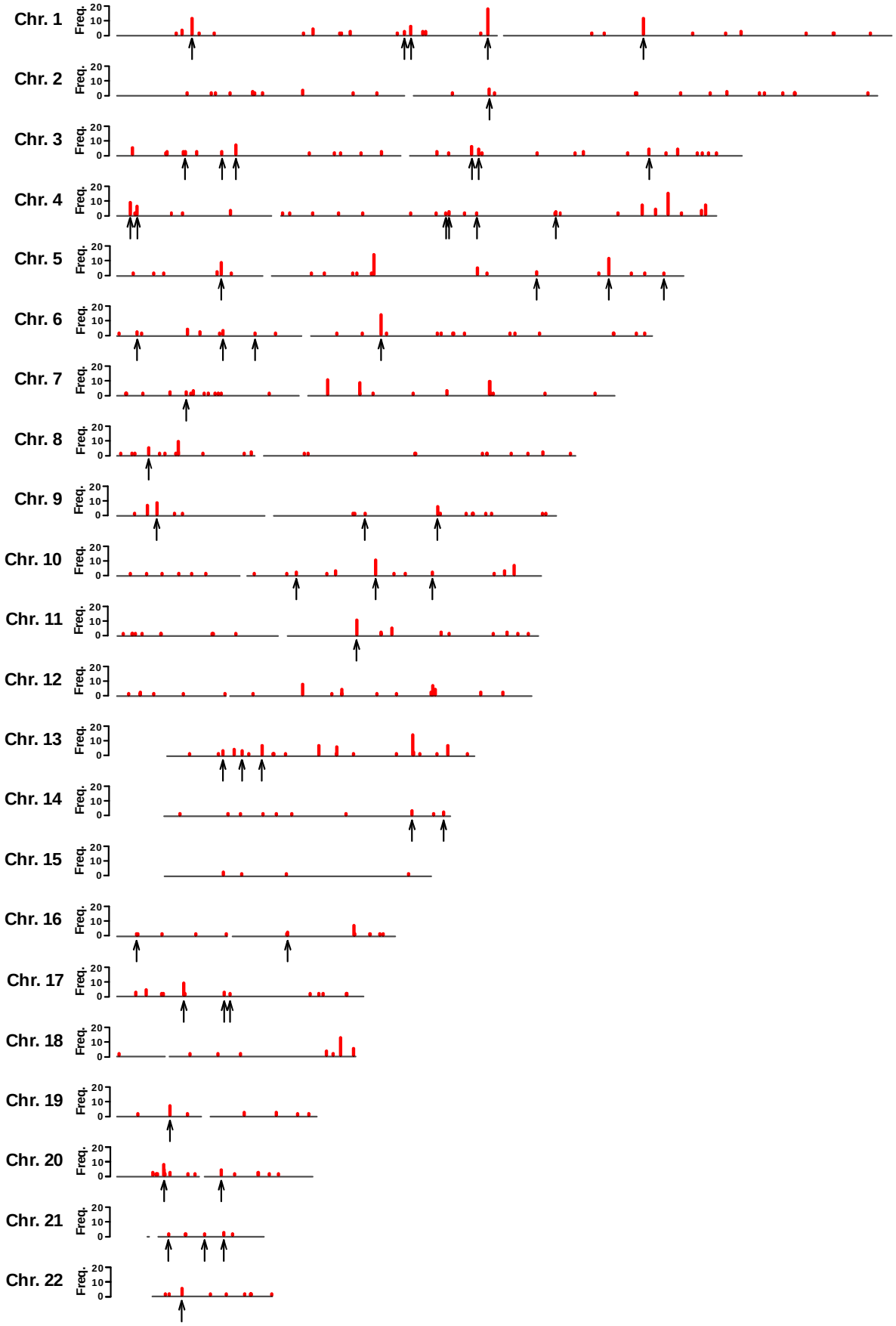
Chr. 1
Freq.
20
10
0
Chr. 2
Chr. 3
Chr. 4
Chr. 5
Chr. 6
Chr. 7
Chr. 8
Chr. 9
Chr. 10
Chr. 11
Chr. 12
Chr. 13
Chr. 14
Chr. 15
Chr. 16
Chr. 17
Chr. 18
Chr. 19
Chr. 20
Chr. 21
Chr. 22

Figure S13. Nonrandom Genome-Wide Distribution of Calls from Small-Scale CNV Analysis using Delta-BAF Filter of 0.2 to 0.45 Combined with Delta-LRR>0.35 between 87 MZ Co-Twins (Figure S1).

Genomic positions (red bars) and frequencies (height of the red bar, maximum 20 occurrences) of 378 putative small-scale CNVs in 87 MZ twin pairs is shown. The data plotted here are derived from Figure 2B and Figure S4D. Black arrows indicate the positions of the 52 CNVs that were validated on the Nimblegen 135K array and which were varying within any of the 34 pairs tested (details shown in Table S4).

Table S1. Summary of findings for monozygotic twins and single-born subjects from ULSAM cohort, which display mega-base range somatic structural genetic variants. The arbitrary limit of large-scale rearrangements has been set at 1 million basepairs (Mb).

Subject ID/ cohort [a]	Age at sampling of blood (years)	Sex	Type, size and position of large-scale somatic genetic aberrations [b]	Platform of primary analysis	Statistical support for Illumina data from primary analysis platform that indicate structural rearrangement [c]	Platforms used for validation experiments	Selected clinical details (age of diagnosis)	Chemo-therapy prior to sampling of blood for the current study	Radio-therapy prior to sampling of blood for the current study	Reference to Figures and Tables in this paper
TP25-2/ MZ twin	70 and 77	female	deletion, 32.46 Mb on 5q, chr. 5: 82822000-115282500; size and position of the deletion is typical for patients with myelodysplastic syndrome	Illumina 600K beadchip	p-value = 1.36 x 10e-214; N-ROI = 5586 SNPs; N-control = 30209 SNPs	Ilumina 1M Omni, Nimblegen 720K, qPCR	dysthymic disorder (60), cholelitiasis (72), cerebral infarction due to thrombosis of cerebral arteries (80), deceased because of cerebral infarction (80).	no	no	Figs. 1 and 5
TP30-1/ MZ twin	69	female	deletion, 12.91 Mb on 20q, chr. 20: 30333600-43245500; size and position of the deletion is typical for patients with myelodysplastic syndrome	Illumina 600K beadchip	p-value = 3.02 x 10e-76; N-ROI = 2284 SNPs; N-control = 12569 SNPs	Ilumina 1M Omni, Nimblegen 720K, qPCR	melaena of uknown cause (79), fracture of the neck of femur (83)	no	no	Figs. 3 and 5
TP12-2/ MZ twin	77	male	terminal CNN-LOH, 76.47 Mb on 10q, chr. 10: 58880000-135347500; copy number imbalance of chromosome Y	Illumina 600K beadchip	p-value = 1.48 x 10e-90; N-ROI = 17169 SNPs; N-control = 13630 SNPs [d]	Ilumina 1M-Omni, Illumina 1M-Duo , Nimblegen 720K	hyperplasia of prostate (66), gastro-esophageal laceration syndrome (Mallory–Weiss syndrome) (79)	no data	no data	Suppl. Fig. 5
D8/ MZ twin [e]	60	female	deletion, 1.62 Mb on 2p, chr. 2: 25312000-26937000	Illumina 600K beadchip	p-value = 2.87 x 10e-38; N-ROI = 56 SNPs; N-control = 15212 SNPs		no data	no data	no data	
292/ MZ twin [e]	80	male	deletion, 22.65 Mb, chr.11, chr. 11: 102626700-125274000; deletion, 86.93 Mb on chr. 4, chr. 4: 1-86929000;	Illumina 600K beadchip	reported previously [e]		Parkinson's disease (68), chronic lymphocytic leukemia (79), deceased (81)	no data	no data	
298/ ULSAM	71 and 88	male	gains and deletions on multiple chromosomes, see Supplementary Figure 7	Illumina IM-Duo beadchip		Illumina 1M-Duo	chronic lymphocytic leukemia with anemia and thrombocytopenia (87), prostate cancer with local spread to lymph nodes (90)	no	no	Suppl. Fig. 10
340/ ULSAM	71, 75 and 88	male	deletion, 13.83 Mb on 20q, chr. 20: 30506000-44334100; size and position of the deletion is typical for patients with myelodysplastic syndrome	Illumina IM-Duo beadchip	p-value < 2.23 x 10e-308; N-ROI = 3449 SNPs; N-control = 15093 SNPs	Illumina 1M-Duo , Illumina Omni-Express, qPCR	malignant cancer of urinary bladder (67), idiopathic thrombocytopenic purpura (87)	no	no	Figs. 4 and 5
697/ ULSAM	71, 82, 88 and 90	male	terminal CNN-LOH, 103.02 Mb on 4q, chr. 4: 88249500-191272500	Illumina IM-Duo beadchip	p-value = 1.614 x 10e-27; N-ROI = 37007; N-control = 31780	Illumina 1M-Duo , Illumina Omni-Express	Colon cancer in sigmoideum treated with surgery (76)	no	no	Fig. 1 and Suppl. Fig. 8
102/ ULSAM	78, 83 and 88	male	gain, 1.09 Mb on 1p, chr. 1: 54842600-55930500; gain, 611.3 kb on 8q, chr. 8: 52422200-53033500;	Illumina IM-Duo beadchip	p-value (1q gain) = 9.46 x 10e-99; N-ROI=682 SNPs; N-control=905 SNPs p-value (8q gain) < 2.23 x 10e-308; N-ROI=208 SNPs; N-control=708 SNPs	Illumina 1M-Duo , Illumina Omni-Express	diffuse large-cell B-cell lymphoma in colon, stage IVA. Treated with partial resection of colon and chemotherapy (82)	yes [f]	no	Fig. 5 and Suppl. Fig. 9

MZ - monozygotic; CNN-LOH - copy number neutral loss of heterozygozity, also called segmental uniparental disomy; Mb - million base pairs.

[a] - description of studied cohorts of monozygotic twins and single-born subjects is provided in Supplemental Table 2.

b - positions of aberrations are according to NCBI36/hg18 genome assembly.

c - Somatic genetic variation in the highlighted regions of interest (ROI) was determined by comparing B allele frequency (BAF) and/or Log R Ratio (LRR) measurements between MZ twin of the same pair for a set of SNP loci. For subjects from ULSAM cohort, the somatic *de novo* nature of the rearrangements was established by examination of samples taken at other time points and comparing BAF and/or LRR measurements between samples at different ages. Significance was calculated by comparing the BAF or LRR differences in twins and ULSAM single born subjects within the ROI and a control region using the Mann-Whitney U test. The control regions for twins TP12-2, TP25-2, TP30-1 and D8 as well as for ULSAM-340 and ULSAM-697 were the remainder of each corresponding chromosome outside the ROI. For smaller aberrations on 1q and 8q in ULSAM-102, 1 million base pairs on both sides of the ROI was selected as control regions.

d - indicate statistical analysis for CNN-LOH aberration on chromosome 10, encompassing approx. 75.5 MB.

e - reported previously in Bruder et al. (ref. [20]).

f - chemotherapy was received prior to sampling of blood at the age of 88.

Table S2 I-X. Summary of somatic mega-base range aberrations detected in the studied cohorts of monozygotic (MZ) twins and single-born subjects. The arbitrary limit of large-scale rearrangements has been set at 1 million basepairs (Mb).

I

All subjects in the study			
	normal	Mb aber.	Total
Young/middle-aged subjects (age ≤55)	342	0	342
Elderly/Old subjects (age ≥60)	255	9	264
All ages	597	9	606

Elderly subjects with mega-base range aberrations (%) 3.4

Fisher's Exact Test; p-value = 0.0005227

II

All Monozygotic twin pairs in the study			
	normal	Mb aber.	Total
Young/middle-aged pairs (age <60)	81	0	81
Elderly/Old pairs (age ≥60)	73	5	78

Fisher's Exact Test; p-value = 0.02656

VIII

All singleborns in the study			
	normal	Mb aber.	Total
Young/middle-aged subjects	180	0	180
Elderly/Old subjects	104	4	108

Fisher's Exact Test; p-value = 0.01909

III

MZ cohort 1: Karolinska Institutet - SATSA [a]			
	normal	Mb aber.	Total
Young pairs	0	0	0
Elderly/Old pairs (age ≥60)	64	3	67

IX

Singleborn cohort 1: Uppsala Univ. - ULSAM [f]			
	normal	Mb aber.	Total
Young subjects	0	0	0
Elderly/Old subjects (age 71-90)	104	4	108

IV

MZ cohort 2: NIH - Autoimmune [b]			
	normal	Mb aber.	Total
Young/middle-aged pairs (age 3-43)	22	0	22
Elderly/Old pairs	0	0	0

X

Singleborn cohort 2: ADVANCE cohort [g]			
	normal	Mb aber.	Total
Young/middle-aged subjects (age 33-55)	180	0	180
Elderly/Old subjects	0	0	0

V

MZ cohort 3: Univ. of Washington [c]			
	normal	Mb aber.	Total
Young pairs (age 18-29)	48	0	48
Elderly/Old pairs	0	0	0

VI

MZ cohort 4: Published in AJHG [d]			
	normal	Mb aber.	Total
Young/middle-aged pairs (age ≤45)	8	0	8
Elderly/Old subjects (age ≥60)	9	2	11

VII

Other MZ twins analysed [e]			
	normal	Mb aber.	Total
Young/middle-aged pairs (age 30-55)	3	0	3
Elderly/Old pairs	0	0	0

Mb aber. - number of subjects with mega-base range aberration
normal - number of subjects with normal profiles

Description of studied cohorts:

[a] Karolinska Institutet - SATSA: The Swedish Adoption Twin Study of Aging (SATSA) is a longitudinal program of gerontological genetics based on all twins in the population based Swedish Twin Regsitry, who were separated before the age of 11 and reared apart and a matched sample of twins reared together. SATSA twins participated in up to 6 waves of questionnaires and 9 waves of in-person testing (IPT) during which a blood sample was collected. For the present investigation, 67 monozygotic pairs over the age of 60 years were selected. For 18 of these pairs, whole blood samples were available from 2 occasions at least 10 years apart and all samples at the second sampling were taken over the age of 60 years. For one additional monozygotic pair, samples available from two time points 7 years apart were also studied.

[b] NIH - Autoimmune: The MZ twin pairs from NIH are a subset of NIH-sponsored study on twins and close siblings discordant for a diagnosis of systemic autoimmune disease. For the present investigation, peripheral blood DNA from 22 young (age 3-43) MZ twin pairs discordant for autoimmune diseases was selected from among a group of 150 pairs who completed the study. Probands meet accepted criteria for adult or juvenile: 1) rheumatoid arthritis; or 2) systemic lupus erythematous; or 3) myositis.

[c] University of Washington: The University of Washington Twin Registry (UWTR) is a community-based registry with a current enrollment of approximately 5 300 twin pairs in Washington State. For the present investigation, monozygotic (MZ) twin pairs were selected from among a group of 226 pairs who completed a study on the genetics of human innate immunity. Participants in that study were generally healthy, had no immune or inflammatory diseases, and were otherwise phenotypically unselected. The 48 pairs randomly selected for this study met the criterion of young age (18-29 years) and uniform European descent ethnicity. Peripheral blood-derived DNA was used for genotyping.

[d] published previously (Bruder et al., ref. [20]).

[e] other MZ twins: two pairs of the MZ twins in this subset are derived from the Norwegian Institute of Public Health/Norwegian Twin Registry. These are normal 37 and 39 year old MZ pairs of healthy controls used in the ongoing project related to genetics of asthma (unpublished). The third pair of MZ twins is derived from Mount Sinai Hospital Medical Center, Chicago, Illinois, USA. This 55 year old MZ twin pair is discordant for the severity of sickle cell disease phenotype. Both MZ twins carry homozygous mutations in the beta-globin gene causing the sickle cell disease (unpublished).

[f] Uppsala University - ULSAM: **U**ppsala **L**ongitudinal **S**tudy of **A**dult **M**en (ULSAM) (http://www2.pubcare.uu.se/ULSAM/index.htm) was started in 1970-1974, when all fifty-year-old men living in Uppsala County, Sweden, were invited to a health survey, initially focusing at identifying risk factors for cardiovascular disease. Out of a total of 2841 men born in 1920-1924, 2322 (82%) agreed to participate in the study. Since then, the cohort has been re-investigated several times. For the present analysis peripheral blood DNA from 108 men were randomly selected from 296 participants of health investigation at 88 years of age. For a few selected cases displaying large-scale genetic changes, DNA obtained at 70, 77, and 82 years investigations was also used. Informed consent from all participating subjects was obtained.

[g] ADVANCE: The dataset is derived from Atherosclerotic Disease, Vascular Function, and Genetic Epidemiology (ADVANCE) study; a genome-wide association analysis of coronary artery disease (refs. [30;31]). The peripheral blood DNA from healthy controls and diseased individuals was collected in Kaiser Permanente clinics in Northern California and at Stanford University, and genotyped on Illumina 550K arrays. We analyzed the LRR and BAF data from 180 control individuals of European descent who had no evidence of cardiovascular disease. The age range for these controls was 33-55 years.

Table S3. Age and Genotyping Quality of 87 MZ Twin Pairs Included in the Aging Analysis Plotted in Figures 2A–2F

Cohort	Twin pair ID	Age at sampling	Genotyping quality twin 1	Genotyping quality twin 2	Difference in genotyping quality between twin 1 and twin 2
NIH - Autoimmune	004-01 / 004-02	43.0	0.02	0.02	0.00
NIH - Autoimmune	010-01 / 010-02	13.0	0.04	0.03	0.01
NIH - Autoimmune	012-01 / 012-02	9.0	0.02	0.03	0.01
NIH - Autoimmune	016-01 / 016-02	34.0	0.02	0.03	0.01
NIH - Autoimmune	030-01 / 030-02	35.0	0.02	0.03	0.01
NIH - Autoimmune	033-01 / 033-02	13.0	0.02	0.02	0.00
NIH - Autoimmune	049-01 / 049-02	20.0	0.02	0.03	0.01
NIH - Autoimmune	061-01 / 061-02	12.0	0.02	0.02	0.00
NIH - Autoimmune	065-01 / 065-02	15.0	0.02	0.04	0.02
NIH - Autoimmune	078-01 / 078-02	8.0	0.03	0.02	0.01
NIH - Autoimmune	079-01 / 079-02	29.0	0.02	0.03	0.00
NIH - Autoimmune	080-01 / 080-02	12.0	0.02	0.02	0.01
NIH - Autoimmune	082-01 / 082-02	19.0	0.02	0.02	0.00
NIH - Autoimmune	085-01 / 085-02	18.0	0.02	0.02	0.00
NIH - Autoimmune	086-01 / 086-02	6.0	0.02	0.03	0.01
NIH - Autoimmune	103-01 / 103-02	3.0	0.03	0.02	0.01
NIH - Autoimmune	112-01 / 112-02	8.0	0.03	0.03	0.00
NIH - Autoimmune	127-01 / 127-02	11.0	0.03	0.02	0.00
NIH - Autoimmune	129-01 / 129-02	5.0	0.02	0.03	0.01
NIH - Autoimmune	132-01 / 132-02	20.0	0.02	0.02	0.00
NIH - Autoimmune	148-01 / 148-02	22.0	0.02	0.02	0.00
NIH - Autoimmune	151-01 / 151-02	6.0	0.02	0.02	0.00
KI - SATSA	TP49A-1 / TP49A-2	69.0	0.07	0.06	0.00
KI - SATSA	TP51A-1 / TP51A-2	68.0	0.05	0.05	0.00
KI - SATSA	TP43B-1 / TP43B-2	82.4	0.05	0.05	0.00
KI - SATSA	TP44B-1 / TP44B-2	82.7	0.05	0.05	0.00
KI - SATSA	TP45B-1 / TP45B-2	82.4	0.07	0.07	0.00
KI - SATSA	TP46B-1 / TP46B-2	80.5	0.05	0.05	0.01
KI - SATSA	TP47B-1 / TP47B-2	80.8	0.07	0.06	0.01
KI - SATSA	TP48B-1 / TP48B-2	79.8	0.05	0.05	0.00
KI - SATSA	TP50B-1 / TP50B-2	78.6	0.05	0.05	0.01
KI - SATSA	TP52B-1 / TP52B-2	78.0	0.06	0.06	0.00
KI - SATSA	TP53B-1 / TP53B-2	76.2	0.06	0.06	0.01
KI - SATSA	TP54B-1 / TP54B-2	68.4	0.08	0.07	0.01
KI - SATSA	TP55B-1 / TP55B-2	65.3	0.06	0.05	0.00
KI - SATSA	TP56B-1 / TP56B-2	66.2	0.05	0.05	0.01
KI - SATSA	TP57B-1 / TP57B-2	65.2	0.05	0.04	0.01
KI - SATSA	TP58B-1 / TP58B-2	64.4	0.04	0.03	0.00
KI - SATSA	TP59B-1 / TP59B-2	63.3	0.04	0.04	0.01
KI - SATSA	TP60B-1 / TP60B-2	62.6	0.03	0.03	0.00

KI - SATSA	TP61B-1 / TP61B-2	60.7	0.06	0.05	0.01
KI - SATSA	TP62B-1 / TP62B-2	75.7	0.05	0.05	0.00
KI - SATSA	TP63B-1 / TP63B-2	76.1	0.06	0.05	0.01
KI - SATSA	TP64B-1 / TP64B-2	75.9	0.07	0.06	0.01
KI - SATSA	TP66B-1 / TP66B-2	75.1	0.05	0.07	0.02
KI - SATSA	TP67B-1 / TP67B-2	75.8	0.04	0.04	0.00
KI - SATSA	TP3-1 / TP3-2	85.9	0.07	0.07	0.00
KI - SATSA	TP5-1 / TP5-2	81.0	0.08	0.08	0.01
KI - SATSA	TP6-1 / TP6-2	81.0	0.06	0.08	0.01
KI - SATSA	TP7-1 / TP7-2	81.0	0.06	0.06	0.00
KI - SATSA	TP8-1 / TP8-2	77.8	0.06	0.06	0.00
KI - SATSA	TP9-1 / TP9-2	78.1	0.05	0.05	0.00
KI - SATSA	TP10-1 / TP10-2	76.5	0.07	0.08	0.01
KI - SATSA	TP11-1 / TP11-2	78.2	0.07	0.07	0.00
KI - SATSA	TP12-1 / TP12-2	77.3	0.07	0.09	0.02
KI - SATSA	TP13-1 / TP13-2	77.0	0.06	0.07	0.01
KI - SATSA	TP14-1 / TP14-2	75.5	0.07	0.07	0.00
KI - SATSA	TP15-1 / TP15-2	75.8	0.07	0.06	0.01
KI - SATSA	TP16-1 / TP16-2	77.3	0.06	0.07	0.00
KI - SATSA	TP18-1 / TP18-2	75.0	0.07	0.07	0.00
KI - SATSA	TP19-1 / TP19-2	74.6	0.09	0.08	0.00
KI - SATSA	TP20-1 / TP20-2	73.0	0.06	0.06	0.01
KI - SATSA	TP21-1 / TP21-2	71.4	0.05	0.04	0.00
KI - SATSA	TP24-1 / TP24-2	71.0	0.05	0.06	0.01
KI - SATSA	TP25-1 / TP25-2	76.7	0.06	0.04	0.02
KI - SATSA	TP26-1 / TP26-2	72.0	0.06	0.06	0.00
KI - SATSA	TP27-1 / TP27-2	69.7	0.07	0.05	0.01
KI - SATSA	TP28-1 / TP28-2	74.4	0.05	0.05	0.00
KI - SATSA	TP29-1 / TP29-2	68.9	0.08	0.07	0.01
KI - SATSA	TP30-1 / TP30-2	68.9	0.08	0.06	0.02
KI - SATSA	TP31-1 / TP31-2	69.0	0.06	0.06	0.00
KI - SATSA	TP33-1 / TP33-2	66.8	0.03	0.04	0.01
KI - SATSA	TP39-1 / TP39-2	66.6	0.03	0.04	0.01
KI - SATSA	TP40-1 / TP40-2	66.4	0.07	0.06	0.01
KI - SATSA	TP41-1 / TP41-2	65.5	0.08	0.09	0.01
KI - SATSA	TP42-1 / TP42-2	68.3	0.09	0.07	0.02
KI - SATSA	TP1-1 / TP1-2	68.0	0.08	0.07	0.00
KI - SATSA	TP34-1 / TP34-2	65.4	0.09	0.09	0.01
KI - SATSA	TP37-1 / TP37-2	64.2	0.07	0.08	0.01
KI - SATSA	TP38-1 / TP38-2	68.7	0.07	0.06	0.01
Univ. Washington	DDS101A / DDS101B	29.0	0.04	0.04	0.00
Univ. Washington	DDS126A / DDS126B	19.0	0.04	0.04	0.00
Univ. Washington	DDS127A / DDS127B	19.0	0.04	0.04	0.00
Univ. Washington	DDS130A / DDS130B	26.0	0.04	0.04	0.00
Univ. Washington	DDS136A / DDS136B	22.0	0.05	0.05	0.00
Univ. Washington	DDS140A / DDS140B	20.0	0.04	0.04	0.00
Univ. Washington	DDS141A / DDS141B	22.0	0.04	0.04	0.00

Genotyping quality was calculated by the Nexus 5 software (Biodiscovery, Inc. CA, USA). Quality criteria for inclusion of pairs in the analysis; NQ < 0.1 for all individuals and maximum NQ difference within pairs of 0.02.

Table S4. Small-scale CNVs validated with the Nimblegen 135K array. The details of 52 loci called by deltaBAF script comparing 87 twin pairs (using parameters: 0.2<deltaBAF<0.45 and deltaLRR>0.35), which were validated using array-CGH hybridization on Nimblegen tiling-path 135K oligonucleotide array, in 34 MZ twin pairs.

SNP name	Chr	Position (NCBI36 / hg18)	Type of aberration as indicated by Illumina genotyping / twin ID	Design window for Nimblegen 135K custom array (NCBI36/hg18) [a]	Number of times loci were validated in any MZ pairs tested (n=34) [b]	Size of a region showing CNV acc. to Nimblegen array (bp) [c]	Genomic position relative to neighboring gene	Official gene symbol	Gene name	Gene Ontology (GO) / Biological process (geneontology.org)	Representative annotations in Genetic Association Database (geneticassociationdb.nih.gov)	Reference to Figures in the current paper
rs2298679	21	34169330	deletion/ TP262	Chr21:34160757-34176363	16	200-2500	intronic	*ITSN1*	Intersectin 1 (SH3 domain protein)	GO:0006897 endocytosis GO:0006915 apoptosis GO:0007242 intracellular signaling cascade GO:0010627 regulation of protein kinase cascade GO:0010647 positive regulation of cell communication GO:0035023 regulation of Rho protein signal transduction GO:0046578 regulation of Ras protein signal transduction GO:0048489 synaptic vesicle transport		Suppl. Fig. 6K
rs329312	5	133928397	deletion/ TP45B-1	Chr5:133922480-133931913	14	120-6700	intronic	*PHF15*	Protein Jade-2 (PHD finger protein 15).	GO:0006325 chromatin organization GO:0016573 histone acetylation		Fig. 5 and Suppl. Fig 6G
rs2295330	1	93809917	deletion/ TP61B-1	Chr1:93792635-93822025	14	100-7000	exonic/prot. coding	*BCAR3*	Breast cancer anti-estrogen resistance protein 3	GO:0007242 intracellular signaling cascade GO:0042493 response to drug		Suppl. Fig. 6H
rs7943716	11	76515147	deletion/ TP61B-2	Chr11:76509459-76518557	13	450-5600	5 prime near gene	*MYO7A*	Myosin VIIA	GO:0006897 endocytosis GO:0009791 post-embryonic development GO:0016192 vesicle-mediated transport GO:0030029 actin filament-based process GO:0033059 cellular pigmentation GO:0042462 eye photoreceptor cell development GO:0042472 inner ear morphogenesis GO:0048598 embryonic morphogenesis GO:0048666 neuron development	131268: Usher syndrome. 131267: hearing loss, sensorineural nonsyndromic.	
rs7140154	14	104234577	deletion/ TP9-2	Chr14:104219500-104239659	12	170-520	intronic	*INF2*	Inverted formin, FH2 and WH2 domain containing	GO:0030036 actin cytoskeleton organization		Suppl. Fig. 6M
rs4841318	8	10224610	deletion/ TP202	Chr8:10223763-10226754	10	270-1600	intronic	*MSRA*	Methionine sulfoxide reductase A	GO:0000096 sulfur amino acid metabolic process GO:0006979 response to oxidative stress GO:0009066 aspartate family amino acid metabolic process GO:0055114 oxidation reduction	598839: obesity. 598840: hypertension. 591255: aging/ Telomere Length.	Fig. 5 and Suppl. Fig. 6J
rs762470	22	20745546	gain/ 126-01	Chr22:20742965-20746773	10	100-1850	intergenic					Suppl. Fig. 6P
rs1122554	6	33906568	gain/ TP62B-1	Chr6:33901993-33912725	9	800-5870	intergenic					
rs7725069	5	156922335	deletion/ TP10-1	Chr5:156898973-156930192	9	500-13000	intronic	*ADAM19*	ADAM metallopeptidase domain 19 (meltrin beta)	GO:0006508 proteolysis GO:0007507 heart development GO:0030163 protein catabolic process	596733: lung diseases.	Suppl. Fig. 6A

rs4635020	10	100703080	gain/ 086-02	Chr10:100694478-100708297	9	550-750	intronic	*HPSE2*	Heparanase 2	GO:0005975 carbohydrate metabolic process		Fig. 2G and Fig. 5
rs2725759	4	105925776	deletion/ TP9-1	Chr4:105919791-105935580	8	760-2420	intergenic					
rs17590228	17	34290556	deletion/ TP38-1	Chr17:34289814-34301384	8	150-3320	intronic	*LASP1*	LIM and SH3 domain protein 1	GO:0006811 ion transport GO:0007010 cytoskeleton organization		
rs4546191	4	140066658	deletion/ TP11-2	Chr4:140058604-140067694	7	330-680	intergenic					Suppl. Fig. 6S
rs1363688	5	174542337	deletion/ TP61B-2	Chr5:174537430-174544755	7	270-3900	intergenic					Suppl. Fig. 6Q
rs7770346	6	44053666	deletion/ TP52B-2	Chr6:44049423-44058119	6	220-3720	intergenic					
rs1014028	4	114807814	deletion/ TP19-2	Chr4:114805049-114813115	6	430-1450	intronic	*CAMK2D*	Calcium/calmodulin-dependent protein kinase type II delta chain	GO:0001666 response to hypoxia GO:0003013 circulatory system process GO:0006468 protein amino acid phosphorylation GO:0006796 phosphate metabolic process GO:0006816 calcium ion transport GO:0006936 muscle contraction GO:0007346 regulation of mitotic cell cycle GO:0008015 blood circulation GO:0008284 positive regulation of cell proliferation GO:0055075 potassium ion homeostasis GO:0060047 heart contraction		Suppl. Fig. 6N
rs9837352	3	37957465	gain/ TP28-1	Chr3:37951504-37961453	6	750-2760	intronic	*CTDSPL*	CTD small phosphatase-like protein		597391: breast and prostate cancers.	Suppl. Fig. 6D
rs7434469	4	6461647	deletion/ 004-01	Chr4:6460249-6467129	5	360-600	intronic	*PPP2R2C*	Serine/threonine-protein phosphatase 2A 55 kDa regulatory subunit B gamma isoform	GO:0007165 signal trasduction	599364: type 2 diabetes and other traits.	Suppl. Fig. 6I
rs2755223	13	39942303	deletion/ TP54B-2	Chr13:39941238-39945268	5	1270-3300	intergenic	*LOC646982*	TTL/TEL fusion protein TTL-B1.			
rs774759	3	113204782	deletion/ TP26-2	Chr3:113202955-113206660	5	340-800	intronic	*TAGLN3*	Transgelin-3	GO:0007517 muscle organ development		
rs10465148	9	102342854	gain/ TP31-2	Chr9:102301849-102367454	5	300-3820	intronic	*TMEFF1*	Transmembrane protein with EGF-like and two follistatin-like domains 1			
rs2462957	17	36095487	deletion/ 086-02	Chr17:36061575-36122206	5	370-670	intergenic					Suppl. Fig. 6E
rs4679072	3	33549244	gain/ TP12-1	Chr3:33530028-33578111	5	480-2000	intronic	*CLASP2*	CLIP-associating protein 2	GO:0007067 mitosis GO:0016477 cell migration GO:0033043 regulation of organelle organization GO:0070507 regulation of microtubule cytoskeleton organization		
rs1606852	3	21812680	deletion/ TP20-1	Chr3:21810800-21817108	5	300-1790	intergenic					
rs2189167	4	104953292	gain/ TP11-1	Chr4:104941311-104955235	4	610-820	intergenic					Suppl. Fig. 6T
rs2076346	1	23956236	gain/ TP1-1	Chr1:23923511-23974867	4	1050-1080	intronic	*TCEB3*	Transcription elongation factor B polypeptide 3	GO:0006351 transcription, DNA-dependent		

rs2916182	5	33293060	gain/ TP28-2	Chr5:33287049-33297208	4	500-620	intergenic					Suppl. Fig. 6B
rs4935610	10	57248430	gain/ TP63B-2	Chr10:57241675-57260771	4	450-1300	intergenic					Suppl. Fig. 6R
rs708039	6	6432930	deletion/ TP63B-1	Chr6:6431584-6440230	4	1180-1400	intronic	*LY86-AS1*	LY86 antisense RNA 1 (non-protein coding)			Fig. 5 and Suppl. Fig. 6O
rs17826697	14	94207226	deletion/ TP19-1	Chr14:94203899-94208624	3	630-2000	intergenic					
rs6928830	6	84276031	deletion/ TP52B-2	Chr6:84271686-84284694	3	530-810	upstream	*PRSS35*	Protease, serine, 35	GO:0006508 proteolysis		Figs. 2H and 5
rs12453531	17	21365866	gain/ TP55B-2	Chr17:21318609-21377374	3	3220-4760	intergenic					
rs1923886	13	46321292	deletion/ TP58B-1	Chr13:46319637-46325827	2	350-1440	intronic	*HTR2A*	5-hydroxytryptamine 2A receptor	GO:0007268 synaptic transmission GO:0007568 aging GO:0042127 regulation of cell proliferation GO:0008219 cell death GO:0010517 regulation of phospholipase activity GO:0043269 regulation of ion transport GO:0014059 regulation of dopamine secretion GO:0019229 regulation of vasoconstriction GO:0042493 response to drug GO:0043405 regulation of MAP kinase activity GO:0051174 regulation of phosphorus metabolic process GO:0051336 regulation of hydrolase activity GO:0051338 regulation of transferase activity GO:0051952 regulation of amine transport GO:0051969 regulation of transmission of nerve impulse GO:0060191 regulation of lipase activity GO:0060341 regulation of cellular localization	581577: ADHD. 126748: Alzheimer's Disease. 126762: bulimia. 126755: depressive disorder. 126787: dyskinesia, Drug-Induced. 126750: irritable bowel syndrome 126718: obesity. 126801: panic disorder. 126752: personality disorders. 149274: schizophrenia.	
rs7042370	9	12775073	gain/ TP20-1	Chr9:12768071-12780701	2	1280-3800	intronic	*C9orf150*	Uncharacterized protein C9orf150.			Suppl. Fig. 6C
rs10882097	10	82558664	gain/ TP11-2	Chr10:82556482-82562289	2	850-1670	intergenic					
rs8105356	19	16917676	deletion/ TP45B-1	Chr19:16901972-16949112	2	8540-16150	intronic	*CPAMD8*	C3 and PZP-like, alpha-2-macroglobulin domain containing 8		597349: Multiple Sclerosis.	
rs8046144	16	6239236	deletion/ TP20-2	Chr16:6237153-6242346	2	1190-1990	intronic	*A2BP1*	Ataxin 2-binding protein 1	GO:0006396 RNA processing GO:0050658 RNA transport GO:0006403 RNA localization	600218: smoking cessation (dependency). 596684: response to antipsychotic therapy (extrapyramidal side effects). 586444: osteoarthritis. 596685: metabolic. 596686: ADHD and conduct disorder.	
rs1431371	21	27971665	gain/ TP28-2	Chr21:27966875-27976776	2	420-1050	intergenic					
rs1833183	16	54482257	gain/ 030-02	Chr16:54473902-54493838	2	1800-4500	intergenic	*CES5A*				
rs2765283	1	118337941	deletion/ TP28-2	Chr1:118327915-118362606	1	610	intronic	*SPAG17*	Sperm associated antigen 17		599725: influence on adult height.	
rs932562	20	33334724	deletion/ TP45B-1	Chr20:33330911-33348769	1	1620	intronic	*EIF6*	Eukaryotic translation initiation factor 6	GO:0042255 ribosome assembly	597519: influence on adult height.	

rs4656703	1	167954759	deletion/ TP44B-1	Chr1:167942717-167963770	1	8600	intergenic					
rs9846423	3	115420025	deletion/ TP19-1	Chr3:115415098-115422134	1	1600	intergenic					
rs1991914	4	4260014	gain/ 101A	Chr4:4258067-4270691	1	1470	intronic	*OTOP1*	Otopetrin 1	GO:0043583 ear development		
rs4814335	20	15001067	gain/ TP52B-2	Chr20:14991423-15004875	1	1660	intronic	*MACROD2*	MACRO domain containing 2 isoform 1			
rs4276037	2	118821447	gain/ 101A	Chr2:118808614-118827516	1	260	intergenic					
rs7630157	3	169797194	gain/ 127-02	Chr3:169785772-169809517	1	200	intronic	*EGFEM1P*	EGFEM1P EGF-like and EMI domain containing 1, pseudogene			Suppl. Fig. 6F
rs1535995	13	33883168	deletion/ TP12-2	Chr13:33880447-33892186	1	270	intergenic					
rs625525	1	91770181	deletion/ TP19-1	Chr1:91758870-91775350	1	5900	intergenic					
rs4722094	7	22098406	deletion/ TP14-1	Chr7:22097746-22104866	1	300	intergenic					
rs11145408	9	79191138	deletion/ TP61B-2	Chr9:79179573-79200947	1	1700	intronic	*VPS13A*	Vacuolar protein sorting-associated protein 13A	GO:0048193 Golgi vesicle transport		
rs2823691	21	16548409	deletion/ TP20-1	Chr21:16540190-16553223	1	270	intronic	*LINC00478*				

[a] - The chromosome segment indicated has been covered by a maximum density of overlapping oligonucleotide probes on the Nimblegen 135K custom array. The overall description of the Nimblegen validation array is provided in Supplemental Figure 6 and Materials and Methods.

[b] - Rows in this Table have been sorted based on the number of times a locus has been validated according to the Nimblegen array experiments, in descending order.

[c] - Range of sizes in base pairs is given when CNVs that were validated on Nimblegen array were not of identical sizes.

Table S5. PCR Primers Used in Real-Time PCR Validation Experiments			
Primer name	Target chromosome	Chromosomal region of PCR product (bp)	Primer sequence (5' -> 3')
UCE3 Forward	3	18819577-18819662	TGGTGCATTCAGTGACCAAA
UCE3 Reverse	3	18819577-18819662	TCTCCAGGGACTGCCTTTATT
UCE6 Forward	6	19666501-19666581	AGGAACAAAATTGGCACCAC
UCE6 Reverse	6	19666501-19666581	GCAATTATGTGACTGCAGGGTA
41.1 Forward	5	110861950-110862042	GGGACATCCAGTTCAGGAAA
41.1 Reverse	5	110861950-110862042	TGAAATTCCAAAGGTGCCTAA
42.1 Forward	5	89845408-89845557	AAGTTGTCATTTGCGGTTGA
42.1 Reverse	5	89845408-89845557	CCTGGTTCAAGTGGTTATCTGC
45.1 Forward	20	33999950-34000065	TCCCCCACTACACGTAACAGT
45.1 Reverse	20	33999950-34000065	GAGTGAGGCTGGGTTAGGTG
46.1 Forward	20	30860119-30860266	CTTTGTGAACGGAAGGCAGT
46.1 Reverse	20	30860119-30860266	CCCCACAGTCTCGACCTCTA
rs540796	1	55296756-55296871	GCAGGTTGGCAGCTGTTT
rs540796	1	55296756-55296871	AAACTGGAGCAGCTCAGCA
rs9298462	8	52908657-52908775	TGCCTCCAACTTTTAGTAATATTTT
rs9298462	8	52908657-52908775	TGTTGGTAATTGCCTCCAGA
rs4635020	10	100702895-100703014	AAGAGAGCTGGGCTTCCTTC
rs4635020	10	100702895-100703014	CACCGAGGAGAACACCAAAT
rs6928830	6	84275967-84276090	ACAGCCAAAGCAATTCAGGT
rs6928830	6	84275967-84276090	TCATGGAAATGTACTTGGAAAGTT
rs4841318	8	10224548-10224700	CCCCATAATCTGGTCTCCAA
rs4841318	8	10224548-10224700	AGTGTGTTCTGGGGTTCAGG
rs329312	5	133928329-133928408	GACTGGGGCCAGAGTCAGA
rs329312	5	133928329-133928408	GGGTCTGTTCCCACTCCCTA
rs708039	6	6432885-6433018	GGGAGAAGAGACACGCTTTG
rs708039	6	6432885-6433018	CTCCCTGAAGAGATGCCTGT

Positions of primers are according to NCBI36/hg18 genome assembly. UCE3 and UCE6 are Ultra Conserved Elements on chromosomes 3 and 6, respectively, which were used as controls.

Table S6. Median BAF Values of Heterozyguous SNPs for Evaluation of Genotyping Quality on Illumina 1M-Duo and Illumina 550K Platform

Cohort	ID	Type of platform	Median BAF values of heterozygote SNPs (Standard deviation)
ULSAM	675	1M-Duo	0.5289 (0.04)
ULSAM	442	1M-Duo	0.5229 (0.0427)
ULSAM	445	1M-Duo	0.5184 (0.0386)
ULSAM	627	1M-Duo	0.5192 (0.0404)
ULSAM	506	1M-Duo	0.5289 (0.0431)
ULSAM	261	1M-Duo	0.4968 (0.0497)
ULSAM	622	1M-Duo	0.5234 (0.0439)
ULSAM	397	1M-Duo	0.5306 (0.0471)
ULSAM	333	1M-Duo	0.5232 (0.041)
ULSAM	296	1M-Duo	0.5242 (0.0447)
ULSAM	504	1M-Duo	0.5255 (0.0486)
ULSAM	555	1M-Duo	0.5251 (0.043)
ULSAM	474	1M-Duo	0.5272 (0.0472)
ULSAM	420	1M-Duo	0.519 (0.0402)
ULSAM	63	1M-Duo	0.5226 (0.0459)
ULSAM	639	1M-Duo	0.5248 (0.0417)
ULSAM	32	1M-Duo	0.5156 (0.0394)
ULSAM	523	1M-Duo	0.497 (0.0444)
ULSAM	102	1M-Duo	0.4972 (0.047)
ULSAM	41	1M-Duo	0.5285 (0.0458)
ULSAM	373	1M-Duo	0.5277 (0.0429)
ULSAM	342	1M-Duo	0.5263 (0.0505)
ULSAM	91	1M-Duo	0.4989 (0.048)
ULSAM	364	1M-Duo	0.5235 (0.0391)
ULSAM	664	1M-Duo	0.5275 (0.0466)
ULSAM	456	1M-Duo	0.5305 (0.041)
ULSAM	648	1M-Duo	0.5245 (0.0479)
ULSAM	73	1M-Duo	0.527 (0.0455)
ULSAM	418	1M-Duo	0.5179 (0.0392)
ULSAM	312	1M-Duo	0.5267 (0.0414)
ULSAM	349	1M-Duo	0.5253 (0.0402)
ULSAM	211	1M-Duo	0.5222 (0.047)
ULSAM	123	1M-Duo	0.5256 (0.0478)
ULSAM	174	1M-Duo	0.5238 (0.0464)
ULSAM	521	1M-Duo	0.5212 (0.0478)
ULSAM	300	1M-Duo	0.5266 (0.0425)
ULSAM	576	1M-Duo	0.5311 (0.0478)
ULSAM	696	1M-Duo	0.5271 (0.0473)
ULSAM	241	1M-Duo	0.532 (0.0465)
ULSAM	711	1M-Duo	0.5252 (0.047)
ULSAM	95	1M-Duo	0.525 (0.038)

ULSAM	697	1M-Duo	0.5255 (0.0462)
ULSAM	621	1M-Duo	0.5249 (0.0442)
ULSAM	498	1M-Duo	0.4953 (0.051)
ULSAM	620	1M-Duo	0.5268 (0.0501)
ULSAM	681	1M-Duo	0.5241 (0.052)
ULSAM	152	1M-Duo	0.5186 (0.0385)
ULSAM	549	1M-Duo	0.5228 (0.0478)
ULSAM	355	1M-Duo	0.5259 (0.0474)
ULSAM	207	1M-Duo	0.4991 (0.0499)
ULSAM	254	1M-Duo	0.5271 (0.0453)
ULSAM	729	1M-Duo	0.5279 (0.0422)
ULSAM	38	1M-Duo	0.5224 (0.0441)
ULSAM	434	1M-Duo	0.5206 (0.0389)
ULSAM	487	1M-Duo	0.496 (0.0429)
ULSAM	114	1M-Duo	0.5223 (0.0381)
ULSAM	674	1M-Duo	0.5239 (0.0472)
ULSAM	209	1M-Duo	0.5279 (0.0419)
ULSAM	346	1M-Duo	0.5268 (0.04)
ULSAM	597	1M-Duo	0.5269 (0.0405)
ULSAM	634	1M-Duo	0.5233 (0.0395)
ULSAM	735	1M-Duo	0.5263 (0.0428)
ULSAM	514	1M-Duo	0.4965 (0.046)
ULSAM	23	1M-Duo	0.5269 (0.0465)
ULSAM	381	1M-Duo	0.5184 (0.0366)
ULSAM	411	1M-Duo	0.5277 (0.0407)
ULSAM	48	1M-Duo	0.4981 (0.0488)
ULSAM	579	1M-Duo	0.5229 (0.0455)
ULSAM	462	1M-Duo	0.4982 (0.0502)
ULSAM	321	1M-Duo	0.5254 (0.0377)
ULSAM	318	1M-Duo	0.524 (0.0422)
ULSAM	590	1M-Duo	0.5276 (0.0396)
ULSAM	686	1M-Duo	0.5258 (0.0438)
ULSAM	452	1M-Duo	0.5207 (0.0376)
ULSAM	298	1M-Duo	0.531 (0.0613)
ULSAM	2	1M-Duo	0.5299 (0.0462)
ULSAM	606	1M-Duo	0.5285 (0.0409)
ULSAM	351	1M-Duo	0.5242 (0.0413)
ULSAM	547	1M-Duo	0.5332 (0.0474)
ULSAM	524	1M-Duo	0.5296 (0.0507)
ULSAM	80	1M-Duo	0.498 (0.0461)
ULSAM	649	1M-Duo	0.5227 (0.0453)
ULSAM	465	1M-Duo	0.5277 (0.0457)
ULSAM	449	1M-Duo	0.5208 (0.0389)
ULSAM	512	1M-Duo	0.5222 (0.0465)
ULSAM	687	1M-Duo	0.5282 (0.0437)
ULSAM	117	1M-Duo	0.5254 (0.0508)

ULSAM	419	1M-Duo	0.4983 (0.0513)
ULSAM	377	1M-Duo	0.5262 (0.0401)
ULSAM	631	1M-Duo	0.5176 (0.0408)
ULSAM	311	1M-Duo	0.5199 (0.042)
ULSAM	408	1M-Duo	0.5266 (0.04)
ULSAM	379	1M-Duo	0.5297 (0.0434)
ULSAM	569	1M-Duo	0.5239 (0.042)
ULSAM	171	1M-Duo	0.5241 (0.0415)
ULSAM	9	1M-Duo	0.4968 (0.0476)
ULSAM	340	1M-Duo	0.5278 (0.04)
ULSAM	43	1M-Duo	0.5186 (0.0382)
ULSAM	153	1M-Duo	0.5264 (0.0496)
ULSAM	668	1M-Duo	0.5176 (0.038)
ULSAM	716	1M-Duo	0.5241 (0.0397)
ULSAM	708	1M-Duo	0.5222 (0.0492)
ULSAM	59	1M-Duo	0.5222 (0.0455)
ULSAM	632	1M-Duo	0.5286 (0.0418)
ULSAM	554	1M-Duo	0.5274 (0.0416)
ULSAM	421	1M-Duo	0.5307 (0.0407)
ULSAM	409	1M-Duo	0.5308 (0.0519)
ULSAM	359	1M-Duo	0.5288 (0.0497)
ADVANCE	R02131	550K	0.5079 (0.0333)
ADVANCE	R02150	550K	0.5045 (0.0363)
ADVANCE	R02161	550K	0.509 (0.0327)
ADVANCE	R02167	550K	0.5107 (0.0302)
ADVANCE	R02169	550K	0.504 (0.0323)
ADVANCE	R02178	550K	0.5145 (0.0376)
ADVANCE	R02179	550K	0.5063 (0.0358)
ADVANCE	R02180	550K	0.5126 (0.0384)
ADVANCE	R02182	550K	0.5061 (0.0343)
ADVANCE	R02190	550K	0.4995 (0.0335)
ADVANCE	R02192	550K	0.4978 (0.0308)
ADVANCE	R02193	550K	0.5038 (0.0323)
ADVANCE	R02202	550K	0.501 (0.0285)
ADVANCE	R02203	550K	0.504 (0.0295)
ADVANCE	R02219	550K	0.5061 (0.0335)
ADVANCE	R02223	550K	0.5083 (0.0315)
ADVANCE	R02232	550K	0.5118 (0.0324)
ADVANCE	R02236	550K	0.5087 (0.0325)
ADVANCE	R02237	550K	0.499 (0.0306)
ADVANCE	R02242	550K	0.5006 (0.0305)
ADVANCE	R02254	550K	0.5122 (0.0318)
ADVANCE	R02257	550K	0.5114 (0.0315)
ADVANCE	R02262	550K	0.5075 (0.0308)
ADVANCE	R02276	550K	0.511 (0.0328)
ADVANCE	R02280	550K	0.5088 (0.0345)

ADVANCE	R02286	550K	0.5095 (0.0321)
ADVANCE	R02290	550K	0.5144 (0.0323)
ADVANCE	R02294	550K	0.511 (0.0391)
ADVANCE	R02295	550K	0.5171 (0.0338)
ADVANCE	R02296	550K	0.513 (0.0332)
ADVANCE	R02300	550K	0.5057 (0.0333)
ADVANCE	R02313	550K	0.5103 (0.0321)
ADVANCE	R02314	550K	0.5105 (0.0301)
ADVANCE	R02315	550K	0.508 (0.031)
ADVANCE	R02322	550K	0.5068 (0.0297)
ADVANCE	R02332	550K	0.5138 (0.0358)
ADVANCE	R02362	550K	0.5099 (0.0309)
ADVANCE	R02367	550K	0.5149 (0.0332)
ADVANCE	R02382	550K	0.506 (0.027)
ADVANCE	R02394	550K	0.5051 (0.0294)
ADVANCE	R02423	550K	0.5184 (0.0329)
ADVANCE	R02459	550K	0.5054 (0.0348)
ADVANCE	R02537	550K	0.5149 (0.0309)
ADVANCE	R02539	550K	0.5156 (0.0386)
ADVANCE	R02549	550K	0.5112 (0.0316)
ADVANCE	R02556	550K	0.5081 (0.0289)
ADVANCE	R02578	550K	0.5098 (0.0307)
ADVANCE	R02601	550K	0.5284 (0.0352)
ADVANCE	R02648	550K	0.5117 (0.0336)
ADVANCE	R02714	550K	0.5066 (0.029)
ADVANCE	R02788	550K	0.5113 (0.0324)
ADVANCE	R02929	550K	0.5155 (0.0344)
ADVANCE	R02941	550K	0.5086 (0.0329)
ADVANCE	R02952	550K	0.5143 (0.0332)
ADVANCE	R02986	550K	0.5105 (0.0345)
ADVANCE	R02987	550K	0.5121 (0.0315)
ADVANCE	R02988	550K	0.5051 (0.0314)
ADVANCE	R02989	550K	0.5081 (0.0328)
ADVANCE	R03004	550K	0.5111 (0.0355)
ADVANCE	R03011	550K	0.5142 (0.0339)
ADVANCE	R03013	550K	0.5113 (0.0347)
ADVANCE	R03015	550K	0.5143 (0.0342)
ADVANCE	R03026	550K	0.5072 (0.033)
ADVANCE	R03027	550K	0.5087 (0.0337)
ADVANCE	R03043	550K	0.5097 (0.0339)
ADVANCE	R03052	550K	0.5046 (0.0296)
ADVANCE	R03054	550K	0.5036 (0.0291)
ADVANCE	R03071	550K	0.5074 (0.0334)
ADVANCE	R03073	550K	0.5088 (0.0394)
ADVANCE	R03085	550K	0.5007 (0.0332)
ADVANCE	R03087	550K	0.505 (0.0376)

ADVANCE	R03092	550K	0.5051 (0.0418)
ADVANCE	RC9003	550K	0.5036 (0.0362)
ADVANCE	RC9005	550K	0.4923 (0.0418)
ADVANCE	RC9012	550K	0.5074 (0.0321)
ADVANCE	RC9013	550K	0.4957 (0.0304)
ADVANCE	RC9014	550K	0.4932 (0.0313)
ADVANCE	RC9018	550K	0.4997 (0.0357)
ADVANCE	RC9025	550K	0.4935 (0.0341)
ADVANCE	RC9031	550K	0.4995 (0.0273)
ADVANCE	RC9032	550K	0.5052 (0.0288)
ADVANCE	RC9033	550K	0.5072 (0.0313)
ADVANCE	RC9035	550K	0.5043 (0.03)
ADVANCE	RC9036	550K	0.497 (0.0314)
ADVANCE	RC9037	550K	0.5034 (0.0305)
ADVANCE	RC9041	550K	0.5042 (0.0318)
ADVANCE	RC9042	550K	0.4948 (0.0271)
ADVANCE	RC9043	550K	0.4932 (0.0258)
ADVANCE	RC9045	550K	0.4987 (0.0294)
ADVANCE	RC9046	550K	0.5092 (0.0329)
ADVANCE	RC9047	550K	0.5045 (0.0298)
ADVANCE	RC9050	550K	0.5018 (0.029)
ADVANCE	RC9051	550K	0.4982 (0.0255)
ADVANCE	RC9054	550K	0.5012 (0.0271)
ADVANCE	RC9055	550K	0.5011 (0.03)
ADVANCE	RC9056	550K	0.5085 (0.031)
ADVANCE	RC9058	550K	0.505 (0.0312)
ADVANCE	RC9067	550K	0.5048 (0.0297)
ADVANCE	RC9068	550K	0.4993 (0.0298)
ADVANCE	RC9069	550K	0.499 (0.03)
ADVANCE	RC9074	550K	0.4996 (0.0292)
ADVANCE	RC9075	550K	0.5067 (0.0343)
ADVANCE	RC9081	550K	0.5051 (0.0346)
ADVANCE	RC9083	550K	0.506 (0.0324)
ADVANCE	RC9085	550K	0.5017 (0.0278)
ADVANCE	RC9086	550K	0.5046 (0.0324)
ADVANCE	RC9088	550K	0.4986 (0.0267)
ADVANCE	RC9089	550K	0.5027 (0.0276)
ADVANCE	RC9090	550K	0.4985 (0.0317)
ADVANCE	RC9096	550K	0.4981 (0.0272)
ADVANCE	RC9101	550K	0.5117 (0.0327)
ADVANCE	RC9105	550K	0.5021 (0.0348)
ADVANCE	RC9106	550K	0.511 (0.0335)
ADVANCE	RC9107	550K	0.5014 (0.0283)
ADVANCE	RC9108	550K	0.5058 (0.0296)
ADVANCE	RC9113	550K	0.5 (0.0294)
ADVANCE	RC9114	550K	0.5017 (0.0281)

ADVANCE	RC9116	550K	0.5028 (0.0278)
ADVANCE	RC9117	550K	0.502 (0.0284)
ADVANCE	RC9118	550K	0.5001 (0.027)
ADVANCE	RC9122	550K	0.4978 (0.0252)
ADVANCE	RC9125	550K	0.4951 (0.0267)
ADVANCE	RC9126	550K	0.4742 (0.0323)
ADVANCE	RC9130	550K	0.5029 (0.0303)
ADVANCE	RC9131	550K	0.5046 (0.0312)
ADVANCE	RC9140	550K	0.503 (0.0369)
ADVANCE	RC9142	550K	0.4999 (0.0296)
ADVANCE	RC9143	550K	0.5041 (0.0374)
ADVANCE	RC9144	550K	0.5044 (0.0298)
ADVANCE	RC9151	550K	0.4931 (0.0302)
ADVANCE	RC9153	550K	0.4944 (0.0274)
ADVANCE	RC9155	550K	0.5042 (0.029)
ADVANCE	RC9163	550K	0.5039 (0.0333)
ADVANCE	RC9164	550K	0.5012 (0.0309)
ADVANCE	RC9165	550K	0.5047 (0.0315)
ADVANCE	RC9166	550K	0.5023 (0.0295)
ADVANCE	RC9168	550K	0.4965 (0.0298)
ADVANCE	RC9169	550K	0.4973 (0.0345)
ADVANCE	RC9176	550K	0.4949 (0.0288)
ADVANCE	RC9184	550K	0.4941 (0.0241)
ADVANCE	RC9189	550K	0.5037 (0.0316)
ADVANCE	RC9192	550K	0.4959 (0.0311)
ADVANCE	RC9196	550K	0.5108 (0.0305)
ADVANCE	RC9201	550K	0.5 (0.0345)
ADVANCE	RC9204	550K	0.503 (0.029)
ADVANCE	RC9205	550K	0.5064 (0.0316)
ADVANCE	RC9207	550K	0.5071 (0.0328)
ADVANCE	RC9210	550K	0.5015 (0.0298)
ADVANCE	RC9215	550K	0.5037 (0.034)
ADVANCE	RC9216	550K	0.5034 (0.0318)
ADVANCE	RC9217	550K	0.5065 (0.0302)
ADVANCE	RC9225	550K	0.5051 (0.0305)
ADVANCE	RC9230	550K	0.5017 (0.0355)
ADVANCE	RC9243	550K	0.498 (0.0307)
ADVANCE	RC9248	550K	0.4982 (0.031)
ADVANCE	RC9250	550K	0.4943 (0.0321)
ADVANCE	RC9252	550K	0.5121 (0.0362)
ADVANCE	RC9257	550K	0.5028 (0.0361)
ADVANCE	RC9258	550K	0.5064 (0.0388)
ADVANCE	RC9259	550K	0.4991 (0.034)
ADVANCE	RC9263	550K	0.5009 (0.0312)
ADVANCE	RC9264	550K	0.4963 (0.0346)
ADVANCE	RC9290	550K	0.5035 (0.0291)

ADVANCE	RC9294	550K	0.5082 (0.0314)
ADVANCE	RC9302	550K	0.5022 (0.0363)
ADVANCE	RC9306	550K	0.4983 (0.0287)
ADVANCE	RC9307	550K	0.4945 (0.0374)
ADVANCE	RC9335	550K	0.5 (0.0354)
ADVANCE	RC9338	550K	0.5025 (0.0322)
ADVANCE	RC9341	550K	0.5034 (0.0358)
ADVANCE	RC9349	550K	0.4944 (0.0303)
ADVANCE	RC9350	550K	0.4968 (0.0371)
ADVANCE	RC9353	550K	0.4959 (0.0358)
ADVANCE	RC9373	550K	0.5073 (0.0323)
ADVANCE	RC9374	550K	0.5031 (0.0295)
ADVANCE	RC9380	550K	0.4988 (0.032)
ADVANCE	RC9386	550K	0.4938 (0.0311)
ADVANCE	RC9475	550K	0.4937 (0.0324)
ADVANCE	RC9477	550K	0.4865 (0.0314)
ADVANCE	RC9478	550K	0.4923 (0.0358)

Table S7. Summary of Genome-Wide Divergence of MZ Co-Twins Derived from Small-Scale *de novo* CNVs that Were Validated on Nimblegen Array

MZ twin PairID / cohort	Age	Number of validated loci on the 135K array	Total size of all loci validated with the 135K array (bp)	Estimated genome-wide CNV divergence between MZ co-twins (%)
TP52B / KI-SATSA	78	32	51040	0.00001646
TP31 / KI-SATSA	69	20	32270	0.00001040
127_X / NIH - Autoimmune	11	13	31700	0.00001022
086_X / NIH - Autoimmune	6	18	27590	0.00000889
126X / Univ. Washington	19	13	24860	0.00000801
TP28 / KI-SATSA	74	18	23470	0.00000757
TP20 / KI-SATSA	75	20	18960	0.00000611
TP66B / KI-SATSA	75	18	18560	0.00000598
TP45B / KI-SATSA	82	4	14810	0.00000477
TP21 / KI-SATSA	71	8	11850	0.00000382
TP5 / KI-SATSA	81	7	10820	0.00000349
TP64B / KI-SATSA	76	1	10620	0.00000342
TP16 / KI-SATSA	77	7	9130	0.00000294
TP11 / KI-SATSA	78	7	7450	0.00000240
030_X / NIH - Autoimmune	35	9	7060	0.00000228
TP26 / KI-SATSA	72	5	5320	0.00000172
TP63B / KI-SATSA	76	6	4670	0.00000151
TP37 / KI-SATSA	64	7	3880	0.00000125
TP33 / KI-SATSA	67	3	3690	0.00000119
TP19 / KI-SATSA	75	4	3230	0.00000104
004_X / NIH - Autoimmune	43	6	2600	0.00000084
151_X / NIH - Autoimmune	6	3	2590	0.00000084
TP3 / KI-SATSA	86	3	2390	0.00000077
TP42 / KI-SATSA	68	2	1980	0.00000064
TP51A / KI-SATSA	68	2	1960	0.00000063
TP61B / KI-SATSA	61	3	1190	0.00000038
TP48B / KI-SATSA	80	1	1170	0.00000038
TP34 / KI-SATSA	65	2	730	0.00000024
130X / Univ. Washington	26	2	630	0.00000020
TP9 / KI-SATSA	78	1	270	0.00000009
TP29 / KI-SATSA	70	1	270	0.00000009
TP13 / KI-SATSA	77	1	240	0.00000008
	median	6	4995	0.00000161

The table is sorted after the total combined size of loci that were differing between MZ co-twins on the 135K array. The percentage was calculated using a total genome size of 3,101,788,170 bp (http://www.ncbi.nlm.nih.gov/projects/genome/assembly/grc/human/data/?build=37).

The total of 34 MZ pairs were included in the validation experiments. For two of these pairs, none of the loci were validated.

Table S8. Age and Genotyping Quality of 18 MZ Twin Pairs in Longitudinal Analyses

Cohort	Twin pair ID	Twins age at sampling A	Twins age at sampling B	Genotyping quality twin 1 sampling A	Genotyping quality twin 2 sampling A	Genotyping quality twin 1 sampling B	Genotyping quality twin 2 sampling B	Difference in genotyping quality between twin 1 and 2 at sampling A	Difference in genotyping quality between twin 1 and 2 at sampling B	Difference in genotyping quality in twin 1 at samplings A and B	Difference in genotyping quality in twin 2 at samplings A and B
KI-SATSA	TP43	72.0	82.4	0.06	0.06	0.05	0.05	0.01	0.00	0.01	0.01
KI-SATSA	TP44	72.7	82.7	0.06	0.05	0.05	0.05	0.00	0.00	0.00	0.00
KI-SATSA	TP45	72.6	82.4	0.08	0.07	0.07	0.07	0.02	0.00	0.01	0.00
KI-SATSA	TP47	71.1	80.8	0.07	0.06	0.07	0.06	0.01	0.01	0.00	0.00
KI-SATSA	TP48	69.9	79.8	0.05	0.06	0.05	0.05	0.00	0.00	0.00	0.00
KI-SATSA	TP50	68.6	78.6	0.05	0.05	0.05	0.05	0.00	0.01	0.00	0.00
KI-SATSA	TP52	68.3	78.0	0.08	0.06	0.06	0.06	0.01	0.00	0.01	0.00
KI-SATSA	TP53	66.2	76.2	0.08	0.06	0.06	0.06	0.02	0.01	0.02	0.01
KI-SATSA	TP55	55.3	65.3	0.05	0.05	0.06	0.05	0.00	0.00	0.01	0.01
KI-SATSA	TP56	56.3	66.2	0.06	0.05	0.05	0.05	0.01	0.01	0.01	0.01
KI-SATSA	TP57	55.1	65.2	0.04	0.04	0.05	0.04	0.00	0.01	0.01	0.00
KI-SATSA	TP58	54.5	64.4	0.04	0.04	0.04	0.03	0.00	0.00	0.00	0.00
KI-SATSA	TP60	52.6	62.6	0.03	0.03	0.03	0.03	0.00	0.00	0.00	0.00
KI-SATSA	TP61	50.7	60.7	0.07	0.06	0.06	0.05	0.01	0.01	0.01	0.01
KI-SATSA	TP62	65.8	75.7	0.06	0.06	0.05	0.05	0.00	0.00	0.01	0.01
KI-SATSA	TP64	65.9	75.9	0.06	0.06	0.07	0.06	0.01	0.01	0.01	0.00
KI-SATSA	TP66	65.3	75.1	0.05	0.05	0.05	0.07	0.00	0.02	0.01	0.02
KI-SATSA	TP67	65.8	75.8	0.04	0.04	0.04	0.04	0.00	0.00	0.00	0.00

Samples collected in the first sampling are denoted as "A" and samples from the second sampling 10 years later are referred to as "B". Genotyping quality was calculated by the Nexus 5 software (Biodiscovery, Inc. CA, USA). Quality criteria for inclusion of pairs in the analysis; NQ < 0.1 for all individuals and maximum NQ difference within pairs of 0.02.